UNCLASSIFIED

AD NUMBER
AD493239
CLASSIFICATION CHANGES
TO: unclassified
FROM: confidential
LIMITATION CHANGES
TO: Approved for public release, distribution unlimited
FROM: Distribution authorized to U.S. Gov't. agencies and their contractors; Administrative/Operational Use; 28 JAN 1953. Other requests shall be referred to Naval Researc Lab., Washington, DC.
AUTHORITY
15 Jan 1958 per Doc Markings; USNRL ltr 14 May 1971

THIS PAGE IS UNCLASSIFIED

[redacted] SECURITY INFORMATION

UNCLASSIFIED

UNANNOUNCED

ASTIA FILE COPY

AD No.

493 239

NRL MEMORANDUM REPORT
No. 116

QUANTITATIVE MEASUREMENTS OF RADAR ECHOES FROM AIRCRAFT
VIII. B-45

W. S. Ament
F. C. MacDonald
H. J. Passerini

RADIO DIVISION I

28 January 1953

NAVAL RESEARCH LABORATORY, WASHINGTON, D.C.

APR 27 1967

UNCLASSIFIED

[redacted]

NOTICE: WHEN GOVERNMENT OR OTHER DRAWINGS, SPECIFICATIONS OR OTHER DATA ARE USED FOR ANY PURPOSE OTHER THAN IN CONNECTION WITH A DEFINITELY RELATED GOVERNMENT PROCUREMENT OPERATION, THE U. S. GOVERNMENT THEREBY INCURS NO RESPONSIBILITY, NOR ANY OBLIGATION WHATSOEVER; AND THE FACT THAT THE GOVERNMENT MAY HAVE FORMULATED, FURNISHED, OR IN ANY WAY SUPPLIED THE SAID DRAWINGS, SPECIFICATIONS, OR OTHER DATA IS NOT TO BE REGARDED BY IMPLICATION OR OTHERWISE AS IN ANY MANNER LICENSING THE HOLDER OR ANY OTHER PERSON OR CORPORATION, OR CONVEYING ANY RIGHTS OR PERMISSION TO MANUFACTURE, USE OR SELL ANY PATENTED INVENTION THAT MAY IN ANY WAY BE RELATED THERETO.

CLASSIFICATION CHANGED TO UNCLASSIFIED

BY AUTHORITY OF ASTIA RECLASS. BULLETIN 5

Date 15 Jan 1958 Signed Richard L. Reedy

OFFICE SECURITY ADVISOR

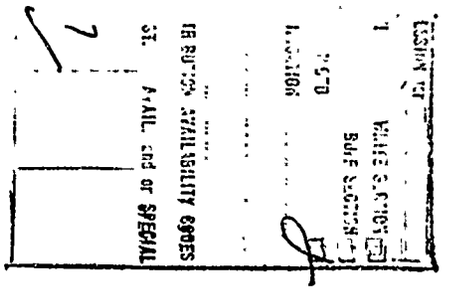

UNCLASSIFIED

[redacted] SECURITY INFORMATION

(6) QUANTITATIVE MEASUREMENTS OF RADAR ECHOES FROM AIRCRAFT VIII. B-45.

[redacted]

(10) W. S. Ament,
F. C. MacDonald
H. J. Passerini

(9) Memorandum rept.,

(11) 28 Jan[redacted]53

(12) 45 pp.

(14) NRL-MR-116

Wave Propagation Research Branch
Radio Propagation-I
Naval Research Laboratory
Washington 25, D. C.

[redacted] UNCLASSIFIED

(251 950)

UNCLASSIFIED

ABSTRACT

B-45 echo amplitudes, sampled over more than four degrees of azimuth, are nearly Rayleigh-distributed for X, S, and L bands.

Averaged over all observed aspects, except the aspect range 85°- 95°, the median radar area of the B-45 is about 12 square meters on all three radar frequencies. Averaged over all observed aspects, the B-45 radar area is about 3 times greater, owing to the large broadside echo.

The aspect diagrams show a relatively wide, high peak at broadside on all three frequencies. Echoes from the leading edges of the wings are prominent at aspects near head-on.

Spectrums of the B-45 echo were obtained for aspects near head-on, near broadside, and toward the tail. A continuous distribution of fluctuation frequencies was found notably in the head-on spectrums, with the significant fluctuation frequencies tending to increase with increase in radar frequency. The near-broadside spectrums are dominated by two discrete fluctuation frequencies probably arising from interference between echoes from the nacelle, the wing tank, and a portion of the fuselage near the tail. This and other features of the B-45 echo behavior are discussed from a theoretical point of view.

PROBLEM STATUS

This is an [redacted] on the problem; work continues.

AUTHORIZATION

NRL Problem R11-17

UNCLASSIFIED

SECURITY INFORMATION

[redacted]

Introduction

In seven previous reports[1),2),3),4),5),6),7)], hereafter referred to as (I), (II), (III), (IV), (V), (VI), and (VII), respectively, some results were given of the measurements of the radar echo characteristics of aircraft made by the Naval Research Laboratory for the Department of the Air Force. (I) and (II) dealt with the approximately head-on runs of six different aircraft. (III) gave the results for the B-36 for the full range of aspects measured. (IV) gave the results for the F-86 for the full range of aspects measured. (V) reported the finding of a source of error in previously published X-band areas, and discussed the procedure to be followed in treating the X-band data in order to obtain valid results. (VI) replaced (IV) and gave the results of the measurements of the radar echo characteristics of the F-86, including corrected X-band areas. (VII) discussed fluctuations of the echo of the B-36 and F-86. This report gives the complete results for the B-45.

Amplitude Distributions

Figs. 2 - 8 consist of cumulative distributions of radar area in decibels above one square meter. Each figure gives the result for ten consecutive seconds (1200 pulses) on the three frequencies employed. The X-band results were corrected in accordance with (V). Most of the distributions fit the theoretical Rayleigh line fairly well. The distributions of Fig. 4 (Run 11) appear to depart farthest from the Rayleigh line and could be better fitted to a line of different slope. It is noted that this sample spans only about two degrees of azimuth, while each of the remaining samples spans more than four degrees of azimuth.

In the discussion of the B-45 data of Figs. 7 and 8 of Report I, it was pointed out that the 2-second samples of B-45 data (spanning about ½ degree of azimuth) were not sufficiently long to produce distributions fitting the Rayleigh. The present 10-second distributions which span more than 4 degrees of azimuth appear to approach a "sufficiently long" span of time. The change in elevation angle was less than one degree for all samples except Fig. 8 (Run 19) which spanned slightly more than one degree. In Fig. 3 (Run 10(b)) and Fig. 5 (Run 14(a)) the X-band distributions curve up sharply away from the Rayleigh line at the high end. These samples were taken from the broadside region. Correction (Report V) . . of the high signals thus encountered necessitated use of the high end of the correction curve, which becomes more critical as the signal level increases. Hence these portions of these distributions probably are not accurate. The plotted points corresponding to weak radar echoes lie to the right of the plots of cumulative distribution and lie above the theoretical straight line fitting the bulk of the points. As this tendency appears to be independent of the percentiles, or abscissas, of the plotted points, it must be attributed to a systematic error arising from the fact that the levels of weak echoes are affected by set noise.

Aspect Dependence

Each of Figs. 9 - 18 covers one flight of the aircraft and consists of four graphs. The uppermost graph of each figure consists of a plot of the aircraft's aspect, as defined in Fig. 1, versus range, in thousands of yards. The remaining three graphs (one for each of the three frequencies

employed) of each figure consist of plots of radar area, expressed in decibels above one square meter, versus range in thousands of yards. Each graph consists of three sets of points, each set being connected by straight line segments. Each point represents one second of data, and data taken simultaneously are aligned vertically so that the uppermost point is the maximum, the middle point is the median, and the lowest point is the minimum radar area occurring in that second. The radar area as plotted contains variations due to interference lobes caused by ground reflections. At the center of each lobe, or integral number of lobes, is a circled x (⊗) indicating the median value (reduced to "free-space" value in accordance with the procedure described in the appendix to (II)) of the median radar area values for that lobe or integral number of lobes, and these median values were used in determining the median value of σ for each five degrees of azimuth as described below.

The data were divided into intervals, each of which spanned five degrees of azimuth. For each such interval the median of the median set of points was determined for each frequency. These "median median" values are plotted in Fig. 19.

Azimuths were originally calculated through the recordings of radar azimuth on the assumption that the B-45 had flown true headings, as instructed. The azimuth of the broadside echo lay at about 100° and there was no symmetry of the aspect pattern about the calculated 0° azimuth. To bring the broadside echo to an azimuth of 90° and to produce symmetry of the aspect pattern about 0° azimuth, all azimuth angles listed in this

B-45 echo amplitudes, sampled over more than four degrees of azimuth, are nearly Rayleigh-distributed for X, S, and L bands. Averaged over all observed aspects, except the aspect range 850-950, the median radar area of the B-45 is about 12 square meters on all three radar frequencies. Averaged over all observed aspects, the B-45 radar area is about 3 times greater, owing to the large broadside echo. The aspect diagrams show a relatively wide, high peak at broadside on all three frequencies. Echos from the leading edges of the wings are prominent at aspects near head-on/ Spectrums of the B-45 echo were obtained formaspects near head-on near broadside, and toward the tail. A continuous distribution of fluctuati on frequencies was dound notably in the head-on spectrums, with the significant fluctuation frequencies tending to increase with increase in raday frequency. The near-broadside spectrums are dominated by two discrete fluctuation frequencies probably arising from interfrrence between echoes from the nacelle, the wing tank, and a portion of the fuselage near the tail. This and other features of the B-45 echo behavior are discussed from a theoretical point of view.

B-2 echo amplitudes, sampled over more than four degrees of azimuth, are nearly Rayleigh-distributed for X, S, and L bands. Averaged over all observed aspects, ~~xxxxpt~~x except the aspect range 850-950, the median radar area of the B-45 is about 12 square meters on all three radar frequencies. Averaged over all observed aspects, the B-45 radar area is about 3 times greater, owing to the large broadside echo. The aspect diagrams show a relatively wide, high peak at broadside on all three frequencies. Echos from the leading edges of the wings are prominent at aspects near head-on. Spectrums of the B-45 echo were obtained frr aspects near head-on near broadside, and toward the tail. A continuous distribution of fluctuation frequencies was found notably in the head-on spectrums, with the significant fluctuation frequencies tending to increase with increase in radar frequency. The near-broadside spectrums are dominated by two discrete fluctuation frequencies probably arising form interference between echoes from a theoretical point of view.

report are 10° less than the corresponding azimuths as calculated originally on the assumption that true headings were flown. Further discussion of this azimuth correction is given in (VI).

The symmetric features of the B-45 aspect pattern about zero degrees of azimuth seem to be produced by echoes from the leading edges of the wings, which are swept back at about 3°. The right leading edge of the wing produces fairly sharp peaks at 355° and 356° azimuth in Fig. 11 (Run 11) and at 355½° in Fig. 12 (Run 13). The left leading edge peaks occur at 6° azimuth in Fig. 17 (Run 19) and at 3½° and 4° in Fig. 18 (Run 20). The two peaks occurring so close together in Fig. 11 and Fig. 18 seem to indicate that the B-45 underwent some yaw oscillations during the flights observed. In these level, straight-line flights, the aspect near zero degrees of azimuth changed so slowly that the leading edge echoes are not sharply defined, so that it was not considered profitable to make a detailed analysis of these echoes, as was done in (VI).

Frequency Dependence

The B-45 X-band data were corrected using the procedure described in (V).

Some of the larger echoes on L and S bands corresponded to the partially-saturated portion of the calibrations used to convert echo amplitudes to decibels. For each calibration on L and S bands there was selected the power level above which the value to be assigned to an echo was indeterminate. Echoes of amplitude greater than this level were not plotted in Figs. 9 - 18, which explains why the tops of some of the broad-

side region data on L and S bands are missing. In most cases enough of the data were present to allow the determination of medians of the median sets of points over five degrees of azimuth. However, for the two azimuth intervals 85°- 90° and 90°-95° on L band, the data were insufficient to allow a satisfactory determination of these medians. Therefore, for the echoes which exceeded the critical power level of the calibration, this level was used as a lower limit in arriving at a "median median" value for the data spanning the particular five degrees of azimuth under consideration.

To obtain representative measures of the radar area of the B-45, the following procedure was carried out for each frequency employed. From Fig. 19, a single number for the radar area was obtained for each five-degree azimuth interval by averaging all the numbers (in square meters) in that azimuth interval, without regard to the elevation angles involved. The results are plotted in Fig. 20. The following four estimates of the average radar area of the B-45 were then obtained, using the results plotted in Fig. 20.

One estimate was obtained by averaging the median radar area, over the azimuth intervals (27 in number, each spanning five degrees) common to all three frequencies employed. This estimate included the azimuth intervals 85°- 90° and 90°- 95°, and the lower limits of the L-band values for these intervals were used in obtaining

the L-band average.

	L	S	X
Square meters	>33.4	29.7	58.6
db > 1 m^2	>15.2	14.7	17.7

When the azimuth intervals 85°- 90° and 90°- 95° were excluded from consideration, a second estimate was obtained by averaging over the remaining azimuth intervals common to the three frequencies employed.

	L	S	X
Square meters	12.5	11.9	11.4
db > 1 m^2.	11.0	10.8	10.6

Comparison of these two estimates illustrates the strong influence of the broadside echoes on the average radar area of the aircraft. As a matter of fact, if, in Fig. 20, the numbers from the azimuth intervals covering from 75°- 105° (or even from 80° - 100°) azimuth are converted to square meters, added, and their sum divided by 27 (the number of azimuth intervals common to all three frequencies), the result for each frequency agrees to within 1 decibel with the result of the first estimate. The broadside echo, therefore, essentially determines the average radar area of this aircraft within the range of aspects (common to all three frequencies) covered.

A third estimate was obtained by calculating, for each frequency employed, the average (in square meters) of all the numbers plotted in Fig. 20. This estimate included the azimuth intervals 85°- 90°, and 90°- 95°, and the lower limits of the L-band values for these intervals were used in obtaining the L-band average.

	L	S	X
Square meters	>31.2	28.0	53.1
db >1 m^2	>14.9	14.5	17.3

When the azimuth intervals 85°- 90° and 90°- 95° were excluded from consideration, a fourth estimate was obtained for each frequency employed by averaging over all the remaining azimuth intervals.

	L	S	X
Square meters	11.7	11.4	10.6
db >1 m^2	10.7	10.6	10.2

The second estimate, being an average of known numbers over azimuth intervals common to all three frequencies employed, is the appropriate measure of the frequency dependence of the average radar area of the aircraft. This estimate indicates that the average radar area is independent of the frequency within the range of frequencies employed, but it is a poor measure of the magnitude of the average radar area.

The first estimate, being an average of numbers, some of which are lower limits, over azimuth intervals common to all three frequencies employed, does not afford as valid a criterion of frequency dependence as does the second estimate, but it is a much better measure of the magnitude of the average radar area. This estimate shows the X-band value to be 3 db greater than the S-band value, while the L-band value is also greater than the S-band value. But, because the L-band value is a lower limit, it cannot be said whether or not the L-band value exceeds the X-band value.

The third and fourth estimates are theoretically poorer for frequency dependence criteria, since they are averages on each frequency over all

the aspects encountered, whereas the first and second estimates are restricted to those azimuths common to all three frequencies employed. Fig. 20 shows that nearly all the aspects encountered have data from all three frequencies. Consequently, the first and third estimates agree very well with each other, as do the second and fourth.

The general conclusion is that the average median radar area of the B-45 is substantially independent of frequency.

Fluctuations of the B-45 Echo

Spectrums of selected 5-second samples of B-45 echoes were prepared according to the procedure described in Report VII. The necessary plots of video voltage vs. time are shown in Figs. 21 - 23, and the spectrums for aspects near head-on, near broadside, and toward the tail are shown in Figs. 24, 25, and 26, respectively.

In the main, these spectrums show a continuous distribution of frequency components in the B-45 echo.* Although the effect is partially obscured by changes of ordinate scale, there is a tendency for higher frequency components to appear in the spectrums as radar frequency increases.

Discrete frequency components (suggested by the similarity in the shape of a portion of the spectrum to the calibration "pulse" found on the right side of each) are found at 2.5 cps in the X-band "tailward" spectrum. The X-band broadside spectrum of Fig. 25 appears to be dominated by two discrete frequencies, at about 5 and 6.6 cps. The spectrum

* It should be noted that the resolution of the spectrum analyzer used makes it impossible to distinguish between a continuous spectrum and a discrete spectrum with component frequencies separated by less than about 1 cps.

analyzer does not quite resolve these into two distinct spikes, as they are separated in frequency by only 1.6 cps.

A frequency component of about 2 cps is discernable on the "tailward" X-band voltage-vs.-time plot of Fig. 23. Likewise, there is obviously a strong fluctuation on the X-band broadside plot of Fig. 22, of order 6 cps, but it is not obvious that there are two distinct frequencies of commensurable amplitudes. On the S- and L-band broadside plots of Figs. 21 and 22, frequencies of order 2 and 1 cps, respectively, seem to be present even though the receiver was saturated part of the time; these low frequencies lie below the cut-off of the spectrum analyzer. (See Fig. 7, Report VII).

Theoretical Picture of the B-45 as a Radar Target

The present measurements were made on a specific large jet aircraft, the B-45, at specific radar frequencies, and for specific flight geometries. By arriving at a consistent explanation of the experimental results through theoretical considerations, a basic understanding of the phenomena involved can be obtained which can be used as a basis for predicting the radar echo behavior of a large jet aircraft in other situations.

In the present data, the principal phenomena requiring explanation are:

(a) The B-45 radar area, averaged over observed non-broadside aspects, is independent of radar frequency.

(b) The B-45 area, averaged over all observed aspects, is independent of frequency (within the probable error of the measurements).

(c) The spectrums are sometimes continuous, and sometimes contain discrete frequency components.

(d) In the case of a continuous spectrum, components are found in higher frequency bands for higher radar frequencies.

(e) Where there is a discrete frequency at, say, f cps in a spectrum made from data at rader frequency F, then, in radar echoes simultaneously observed at radar frequency F', there is, in general, a discrete frequency component at frequency $f' = (F'/F)f$ cps.

(f) In samples spanning more than four degrees of azimuth, the B-45 echo is Rayleigh-distributed.

These phenomena can be explained in terms of a rigidly connected arrangement of reflecting objects of various sizes, shapes, and locations, with one large, approximately cylindrical object corresponding to the fuselage, which dominates the echo at broadside aspect. It is well known that the average radar area of a single large convex metal object is proportional to the average area of the shadow that would be cast by the object, both averages being taken over all possible orientations of the object in space. In the B-45 echo at non-broadside aspects, one can assume that, for the individual objects causing the echo, the measurements span a sufficient band of aspects that the foregoing rule holds for each particular object. Furthermore, one may assume that, over a wide band of non-broadside aspects, the individual echoes add at the radar with all combinations of relative phases, so that the average total echo power is equal to the sum of the individual average echo powers. Then it follows that the sum of the frequency-independent average powers is independent of frequency. The large cylindrical object corresponding to the fuselage itself has a frequency-independent average echo.

(d) In the case of a continuous spectrum, components are found in higher frequency bands for higher radar frequencies.

(e) Where there is a discrete frequency at, say, f cps in a spectrum made from data at radar frequency F, then, in radar echoes simultaneously observed at radar frequency F', there is, in general, a discrete frequency component at frequency $f' = (F'/F)f$ cps.

(f) In samples spanning more than four degrees of azimuth, the B-45 echo is Rayleigh-distributed.

These phenomena can be explained in terms of a rigidly connected arrangement of reflecting objects of various sizes, shapes, and locations, with one large, approximately cylindrical object corresponding to the fuselage, which dominates the echo at broadside aspect. It is well known that the average radar area of a single large convex metal object is proportional to the average area of the shadow that would be cast by the object, both averages being taken over all possible orientations of the object in space. In the B-45 echo at non-broadside aspects, one can assume that, for the individual objects causing the echo, the measurements span a sufficient band of aspects that the foregoing rule holds for each particular object. Furthermore, one may assume that, over a wide band of non-broadside aspects, the individual echoes add at the radar with all combinations of relative phases, so that the average total echo power is equal to the sum of the individual average echo powers. Then it follows that the sum of the frequency-independent average powers is independent of frequency. The large cylindrical object corresponding to the fuselage itself has a frequency-independent average echo.

If the average shadow area of this object is large compared with the sum of similar areas for the other echoing objects, then the average radar area, taken over all aspects, is an area depending primarily on the fuselage, and should be frequency-independent. Finally, the echo from the fuselage is powerful only near the broadside aspect. Thus, for the fuselage, integrating the radar echo power over a narrow band of broadside aspects gives substantially the same total power as integrating it over all aspects.

The total integrated B-45 area thus comprises a frequency-independent sum over non-broadside aspects, plus a frequency-independent sum over a narrow band of broadside aspects. It follows that the average B-45 radar area is frequency-independent, whether broadside aspects are, or are not, included in the average. This explains (a) and (b). The magnitude of the average area, of course, is different in the two cases.

In the radar echo, fluctuations are caused when the rigidly connected echoing objects, under change in B-45 aspect, change in relative distance from the radar so that the phase relations change among the several echo contributions. For any two component echoes, the rate of change of relative phase, $d\phi/dt$, is given (in radians per second) by

$$d\phi/dt = 4\pi\left[\left(\vec{D}/\lambda\right)\times\vec{r}\right]\cdot\vec{\omega} \qquad (1)$$

where $\vec{D}$ is the vector separating the two echoing objects, $\vec{\omega}$ is the axial vector representing the instantaneous rate of change of B-45 aspect (in radians per second), $\vec{r}$ is a unit vector in the direction of the radar rays, λ is the radar wavelength, $(\times)$ and $(\cdot)$ symbolize the vector and scalar product, respectively. From this it is obvious that fluctuation rates

observed simultaneously on different radar frequencies are proportional to radar frequency, as well as to the angular turning rate of the aircraft. This explains (e).

A continuous distribution of component frequencies in the echo spectrum (or a large number of comparable discrete frequencies not individually resolvable by the spectrum analyzer) would be caused by the presence of large numbers of relative rates of change of phase among the individual echoers: if there are N echoers, there are N(N - 1) possible simple beat frequencies (not counting possible beats with the pulse frequency of the radar or possible redundancies). Thus one may account for a continuous contribution of frequencies in the B-45 echo by assuming that the echo arises from a large number of different points on the B-45; an additional consideration tending to make the echo more "random" and the spectrum more continuous is the fact that amplitudes, as well as relative phases, of the individual echoes change with aspect change. This explains (c) and (d).

It is well known that a radar echo arising from a large number of scattering objects is Rayleigh-distributed, provided that the individual echoes undergo a sufficiently wide variety of relative phases during the period in which the echo is sampled. If the collection of objects comprising the B-45 as a radar echoer are spread somewhat uniformly over a horizontal area about 40 L-band wavelengths (32 feet) in diameter, then the average change of relative phase between two echoers in a four-degree aspect change is of the order 2π radians. On the assumption that this guarantees a "sufficiently wide variety of relative phases" in the L-band

echo, (f) is explained; for the relative phase change should be proportionately greater at the higher S- and X-band frequencies.

To explain the echo behavior more quantitatively, one must correlate the echoing objects with particular parts of the aircraft, taking account of individual shapes and spacings. (For the F-86, the leading edge of the wing was discussed in detail as an individual echoing object in Report VII. Mention was also made of the echo behavior caused by the tapering of the fuselage near the F-86 tail.). The leading edge of the B-45 wing produces a sharp echo, but the details of this echo are not prominent in a 5-second sample owing to the slow angular rates of the B-45 at this aspect.

In a semi-quantitative way, one may account for the X-band broadside spectrum of Fig. 25, which consists primarily of two discrete frequencies of about equal amplitude at frequencies 5 and 6.6 cps. The azimuth aspect change during the five-second period sampled was a nominal 2.75°, (assuming no yaw rate), so that the angular turning rate was about 0.01 radian per second. The average observed azimuth was about 97½°; with the aid of a protractor and a plan drawing of the B-45, one finds that surfaces of the port wing tank, the port nacelle, and a curving portion of the fuselage near the tail are normal to the radar rays at azimuth 97½°. According to the outline drawing of the B-45, the nacelle and the wing tank should have about the same radar area at this aspect. Further, according to this drawing, a radar ray normal to the fuselage (near the tail) is about 300 X-band wavelengths away from a ray normal to the nacelle's surface and about 400 wavelengths away from the parallel ray normal to the wing tank.

(These numbers are equivalent to $\left|(\vec{D}/\lambda) \times \vec{r}\right|$ in (1).). Thus interference between the nacelle and fuselage echo should produce a beat frequency of approximately 6 cps in the radar echo; the combination of wing tank and fuselage echo should produce an 8 cps frequency, and the combination of wing tank and nacelle, a 2 cps frequency. On the assumption that the near-tail fuselage echo amplitude is considerably larger than the (roughly commensurate) echoes from nacelle and wing tank, the amplitude of the 2 cps frequency should be relatively small compared with the predicted 6 and 8 cps frequencies, and therefore not discernable to the eye on the voltage-vs.-time plot of Fig. 22.* The observed frequencies 5 and 6.6 cps are in general accord with this "prediction"; i.e. $5/6.6 \approx 6/8$. The fact that the observed frequencies are roughly 5/6 of the ones "predicted" can be explained by assuming that, in the 5 seconds of radar observation, an appropriate small yaw rate of the B-45 occurred. The yaw rate required is only 0.14°/sec.

*A 2 cps frequency would not pass the spectrum analyzer; hence, it is not found in Fig. 25, either.

Conclusions

B-45 echo amplitudes, sampled over more than four degrees of azimuth, are nearly Rayleigh distributed for X, S, and L bands.

Averaged over all observed aspects, except the aspect range 85°- 95°, the median radar area of the B-45 is about 12 square meters on all three radar frequencies. Averaged over all observed aspects, the B-45 radar area is about 3 times greater, owing to the large broadside echo.

The aspect diagrams show a relatively wide, high peak at broadside on all three frequencies. Echoes from the leading edges of the wings are prominent at aspects near head-on.

Spectrums of the B-45 echo were obtained for aspects near head-on, near broadside, and toward the tail. A continuous distribution of fluctuation frequencies was found notably in the head-on spectrums, with the significant fluctuation frequencies tending to increase with increase in radar frequency. The near-broadside spectrums are dominated by two discrete fluctuation frequencies, probably arising from interference between echoes from the nacelle, the wing tank, and a portion of the fuselage near the tail.

Much of the observed dynamic behavior of the B-45 radar echo can be explained by a simple theory in which the B-45 is regarded as a rigidly connected set of echoing objects, including a large, approximately cylindrical, object corresponding to the fuselage. By this theory, one can predict radar echo behavior in other situations.

References

1) "Quantitative Measurements of Radar Echoes from Aircraft, I. B-36, B-45, F-51, and F-86," NRL Letter Report, Serial C-3460-73A/50 dtd 24 October 1950.

2) "Quantitative Measurements of Radar Echoes from Aircraft, II. Formation of Three F-86's, B-29, F-80 with wing tanks, and F-80 without wing tanks", NRL Letter Report, Serial C-3460-18A/51 dtd 12 February 1951.

3) "Quantitative Measurements of Radar Echoes from Aircraft, III. B-36 Amplitude Distributions and Aspect Dependence," NRL Letter Report, Serial C-3460-94A/51 dtd 19 June 1951.

4) "Quantitative Measurements of Radar Echoes from Aircraft, IV. F-86 Amplitude Distributions and Aspect Dependence, " NRL Letter Report, Serial C-3460-138A/51 dtd 5 September 1951.

5) "Quantitative Measurements of Radar Echoes from Aircraft, V. Correction of X-band Values," NRL Letter Report, Serial C-3460-132A/52 dtd 24 October 1952.

6) "Quantitative Measurements of Radar Echoes from Aircraft, VI. Corrected F-86 Amplitude Distributions and Aspect Dependence," NRL Letter Report, Serial C-3460-143A/52 dtd 15 December 1952.

7) "Quantitative Measurements of Radar Echoes from Aircraft, VII. B-36 and F-86 Spectrums," NRL Memorandum Report No. 107.

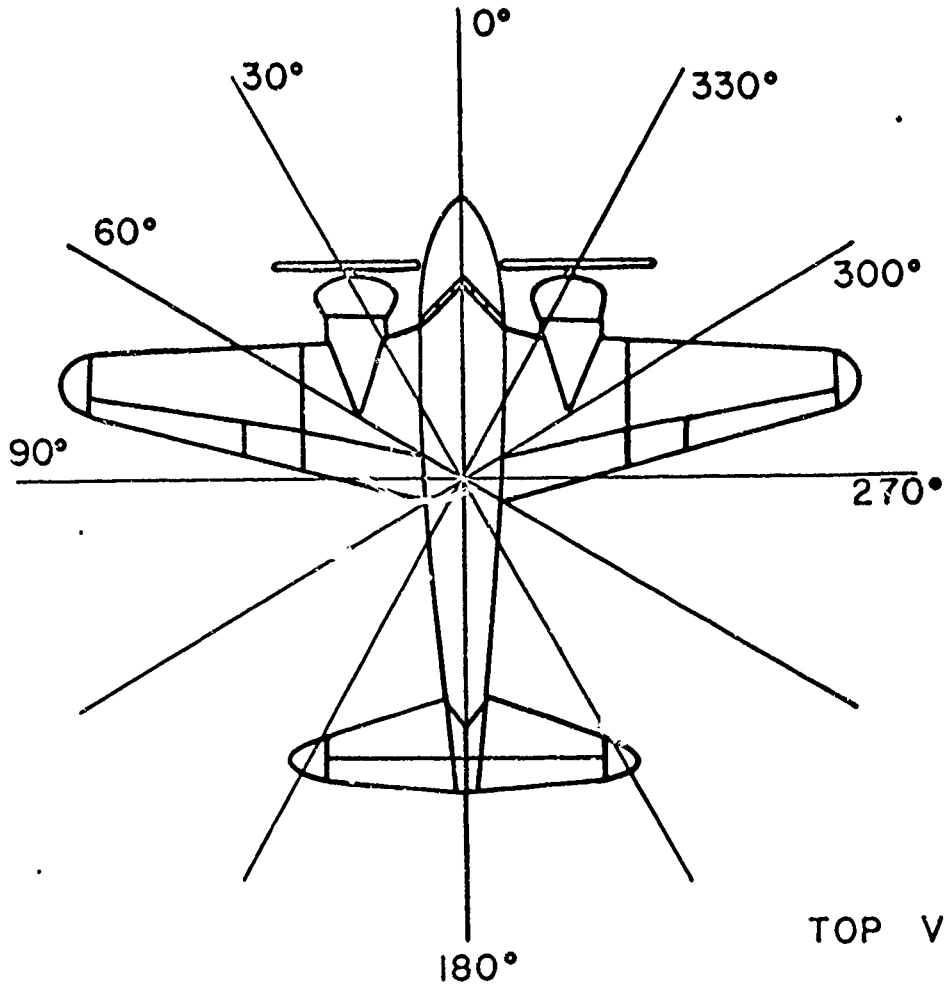

TOP VIEW

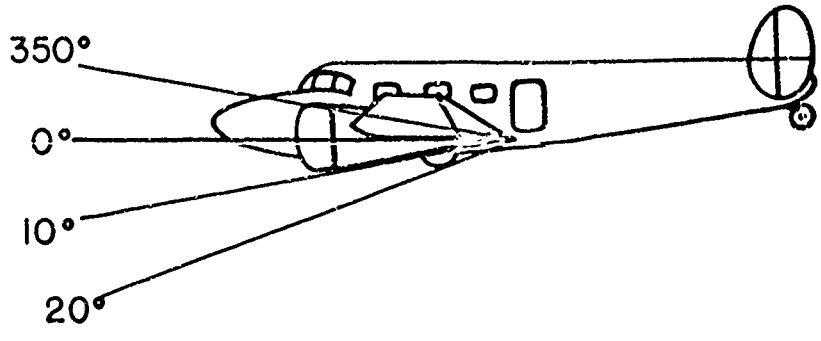

Definition of aspect angles

Figure 1

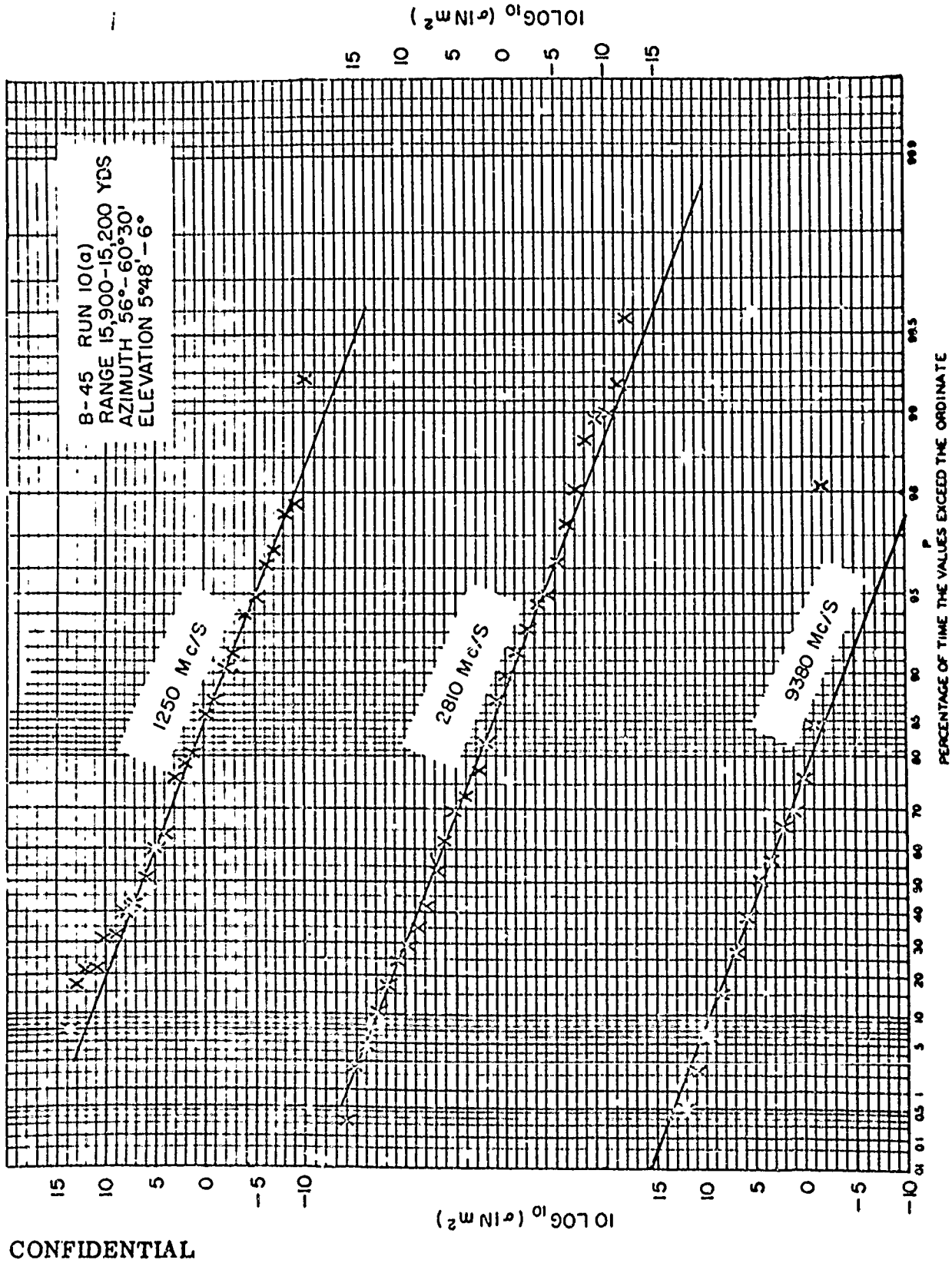
B-45 RUN 10(a)
RANGE 15,900-15,200 YDS
AZIMUTH 56°-60°30'
ELEVATION 5°48'-6°
1250 Mc/S
2810 Mc/S
9380 Mc/S
10 LOG10 (σ IN m²)
PERCENTAGE OF TIME THE VALUES EXCEED THE ORDINATE

Figure 2

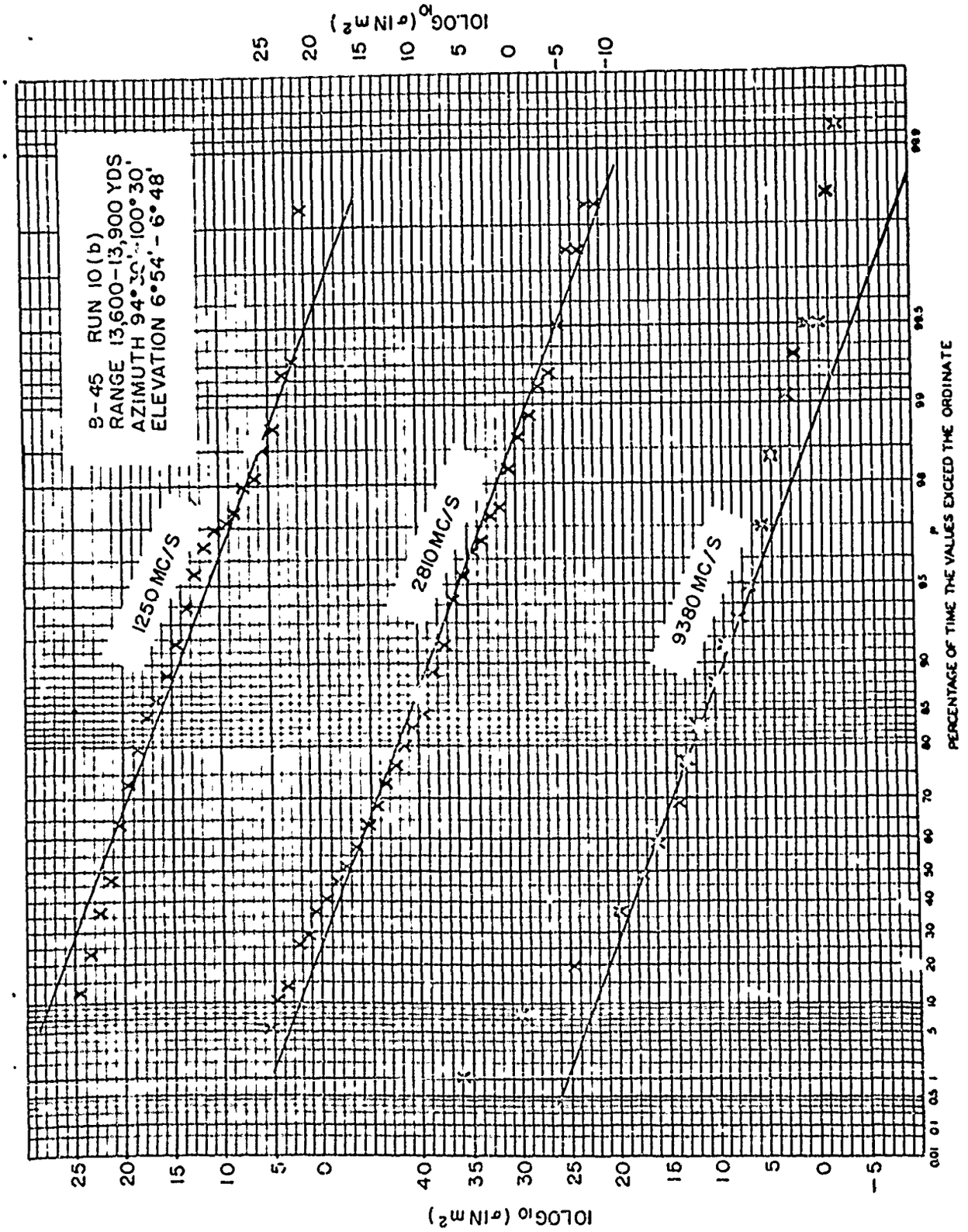
B-45 RUN 10(b)
RANGE 13,600-13,900 YDS
AZIMUTH 94°30'-100°30'
ELEVATION 6°54'-6°48'
1250 MC/S
2810 MC/S
9380 MC/S
PERCENTAGE OF TIME THE VALUES EXCEED THE ORDINATE
10LOG10 (σ IN m²)
10LOG10 (σ IN ft²)

Figure 3

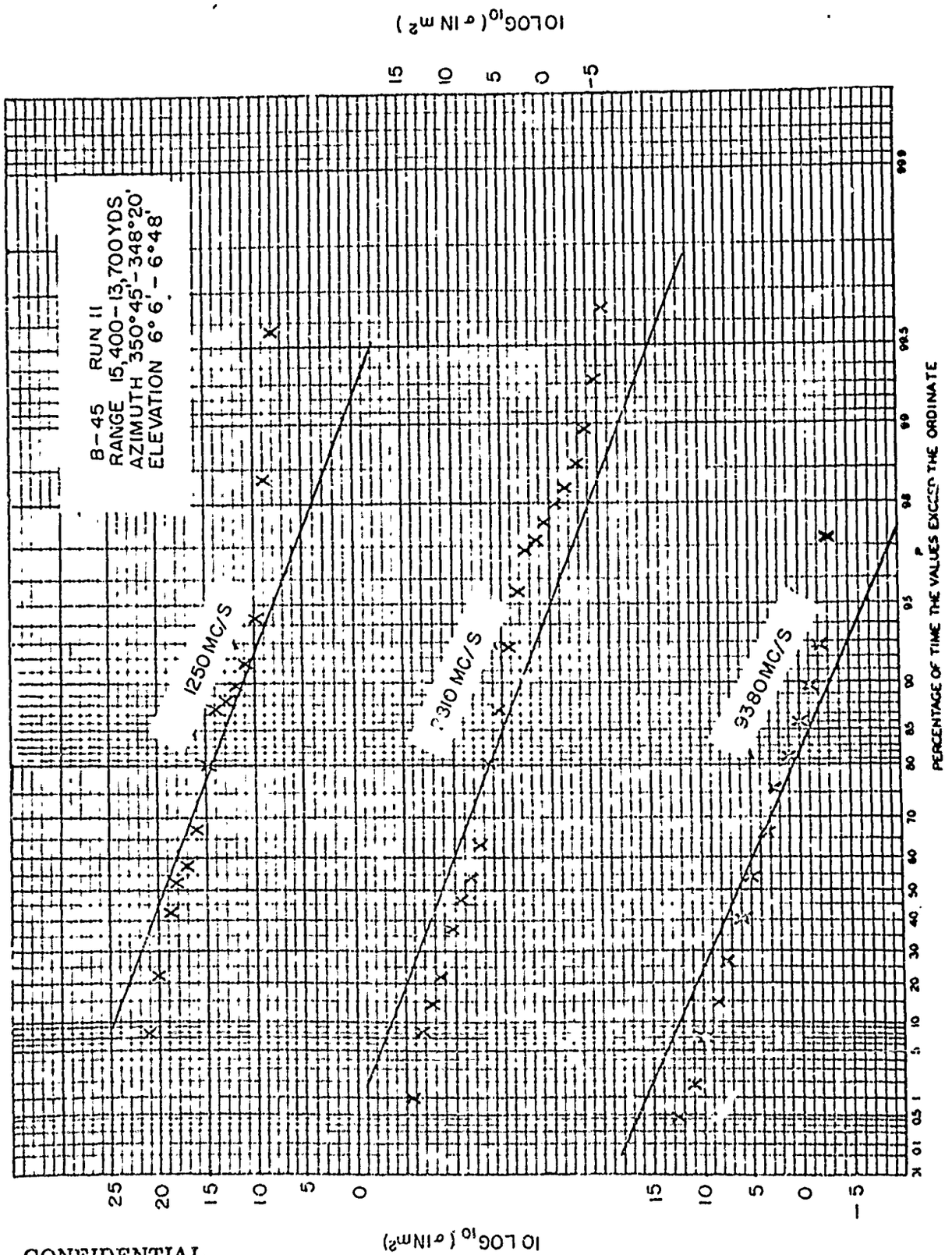
B-45 RUN 11
RANGE 15,400-13,700YDS
AZIMUTH 350°45'-348°20'
ELEVATION 6°6'-6°48'
1250MC/S
9380MC/S
10LOG10(σ IN m²)
PERCENTAGE OF TIME THE VALUES EXCEED THE ORDINATE

Figure 4

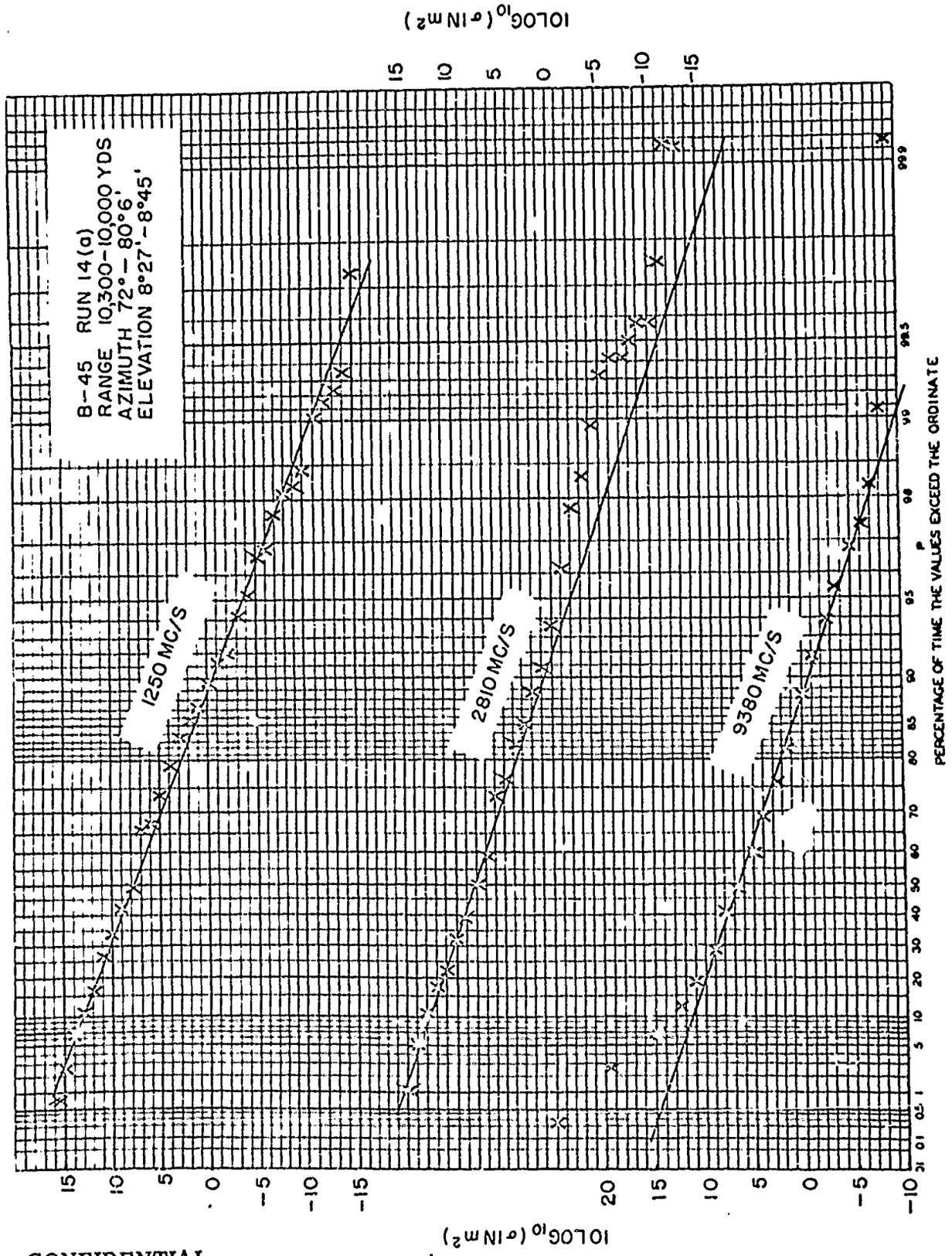
B-45 RUN 14(a)
RANGE 10,300-10,000 YDS
AZIMUTH 72°-80°6'
ELEVATION 8°27'-8°45'
1250 MC/S
2810 MC/S
9380 MC/S
10LOG10 (σ IN m²)
PERCENTAGE OF TIME THE VALUES EXCEED THE ORDINATE

Figure 5

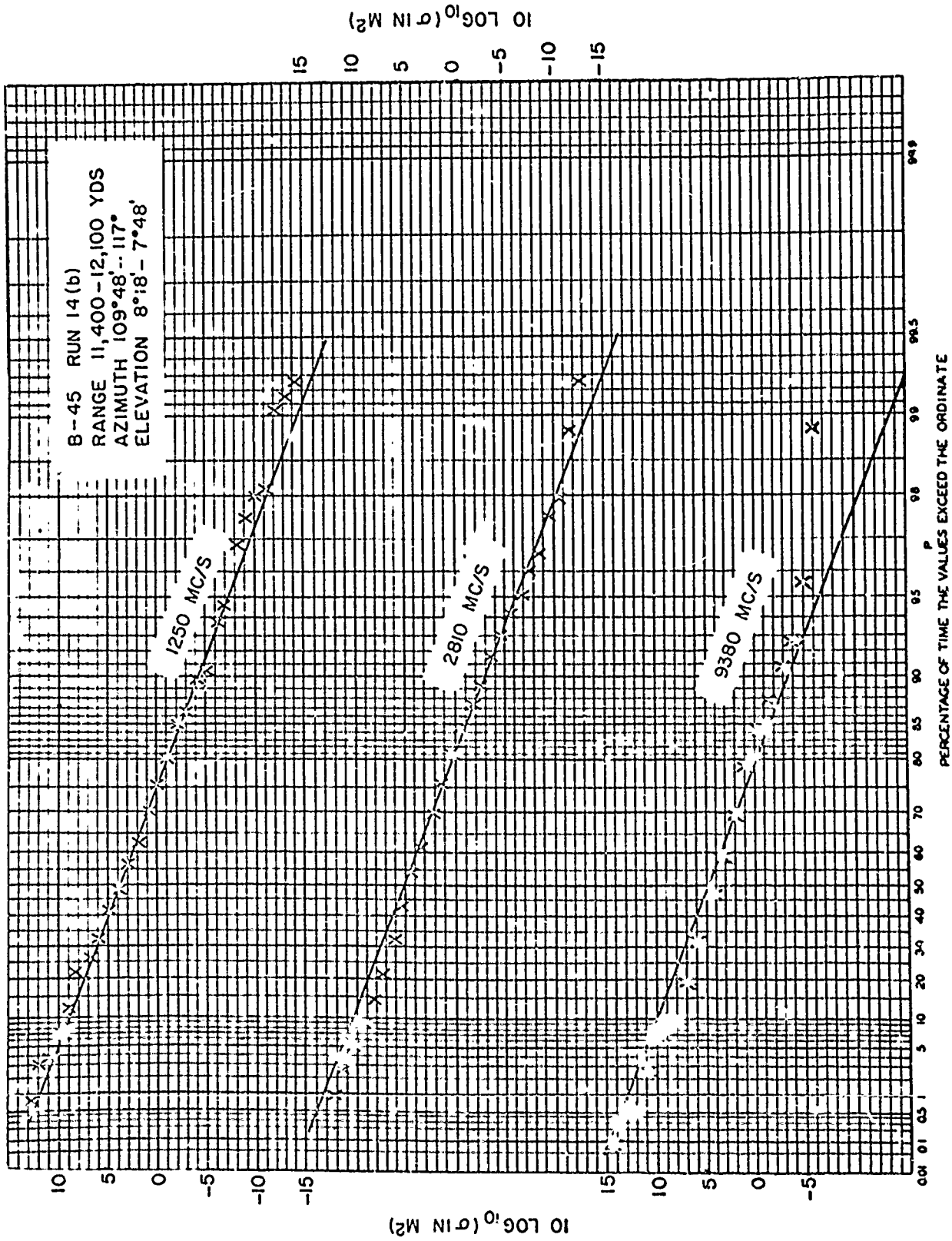
B-45 RUN 14(b)
RANGE 11,400-12,100 YDS
AZIMUTH 109°48'-117°
ELEVATION 8°18'-7°48'
1250 MC/S
2810 MC/S
9380 MC/S
10 LOG10(σ IN M2)
PERCENTAGE OF TIME THE VALUES EXCEED THE ORDINATE

Figure 6

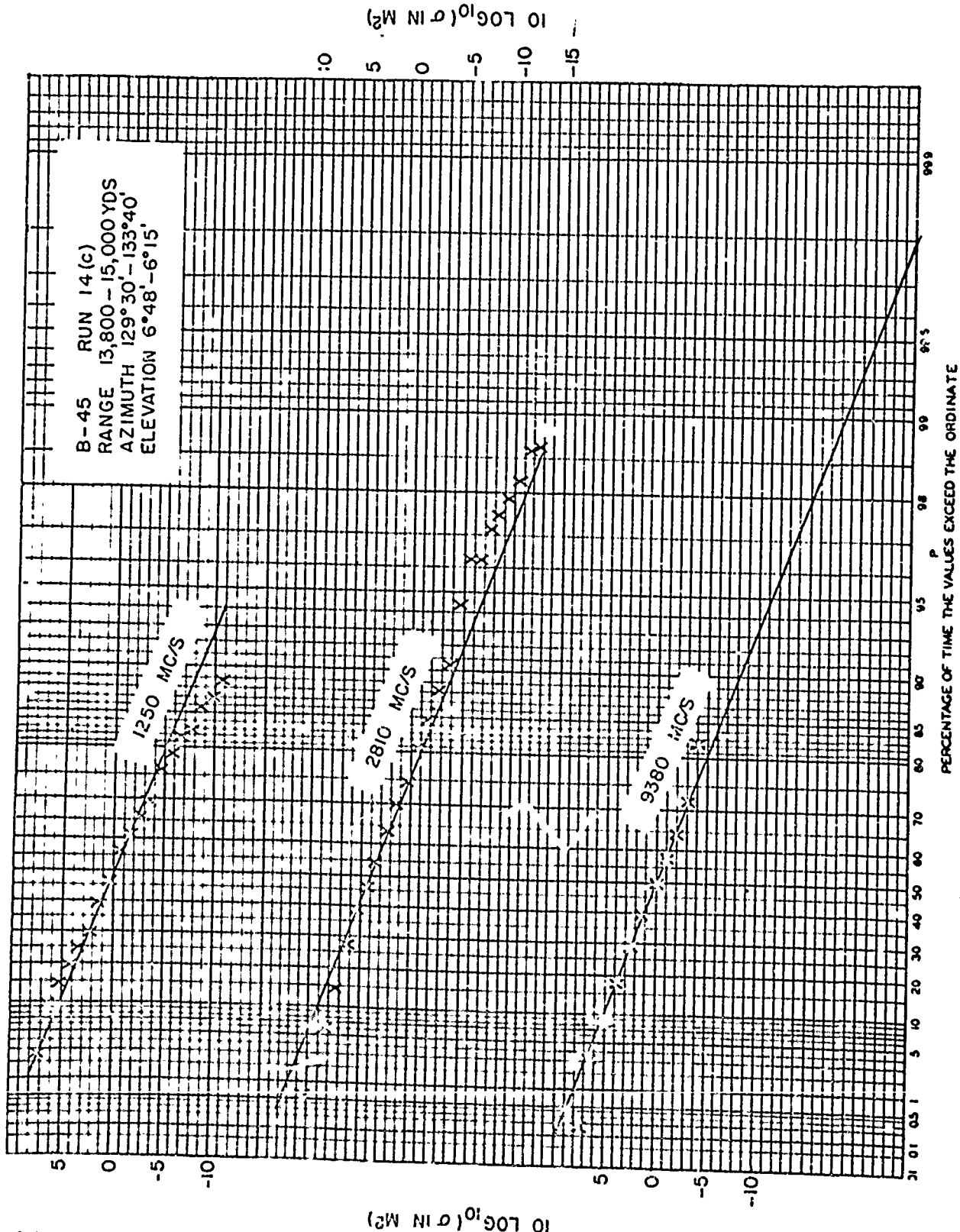
10 LOG10(σ IN M2)
B-45 RUN 14(c)
RANGE 13,800-15,000 YDS
AZIMUTH 129°30'-133°40'
ELEVATION 6°48'-6°15'
1250 MC/S
2810 MC/S
9380 MC/S
PERCENTAGE OF TIME THE VALUES EXCEED THE ORDINATE

Figure 7

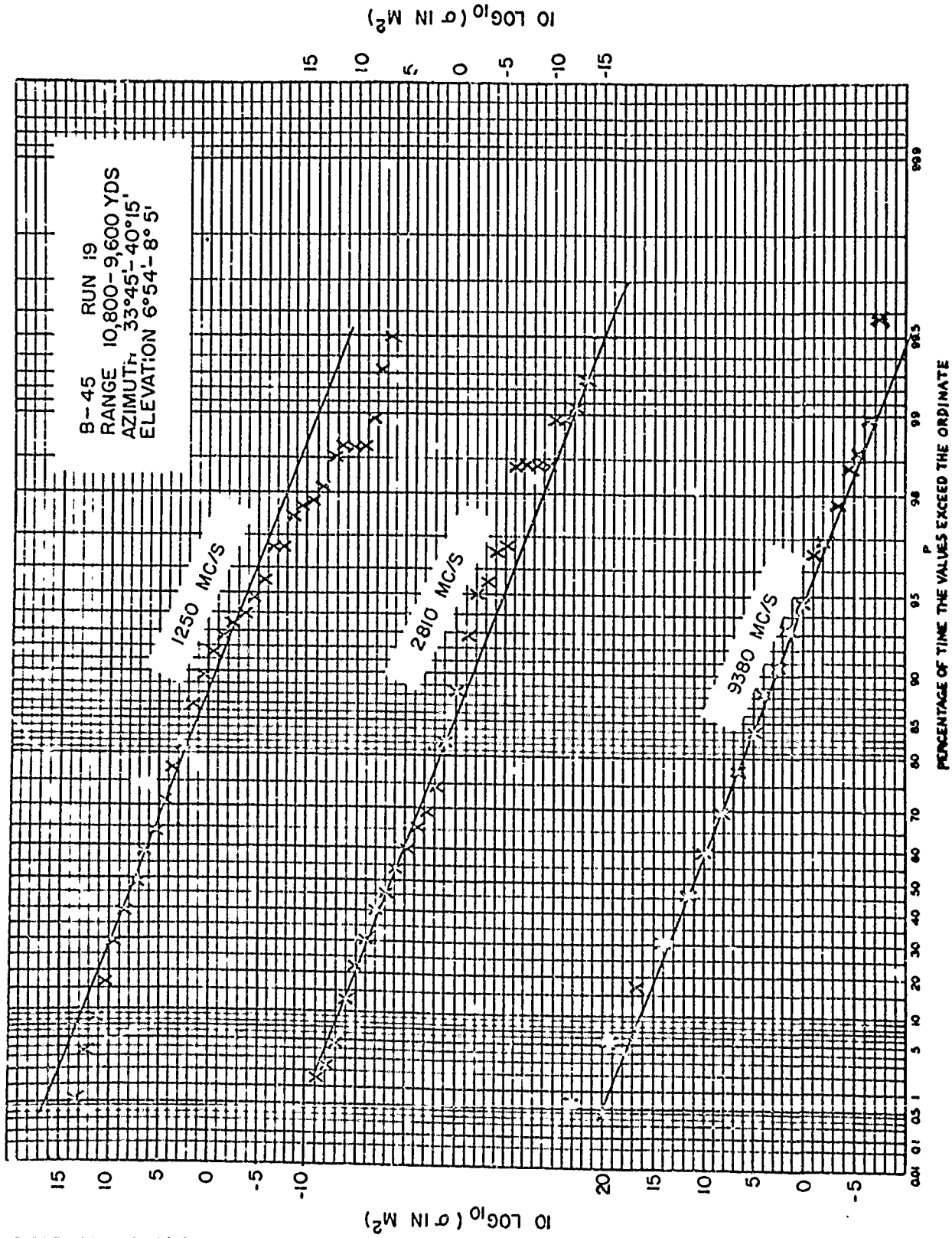
B-45 RUN 19
RANGE 10,800-9,600 YDS
AZIMUTH 33°45'-40°15'
ELEVATION 6°54'-8°5'
1250 MC/S
2810 MC/S
9380 MC/S
10 LOG10 (σ IN M2)
PERCENTAGE OF TIME THE VALUES EXCEED THE ORDINATE

Figure 8

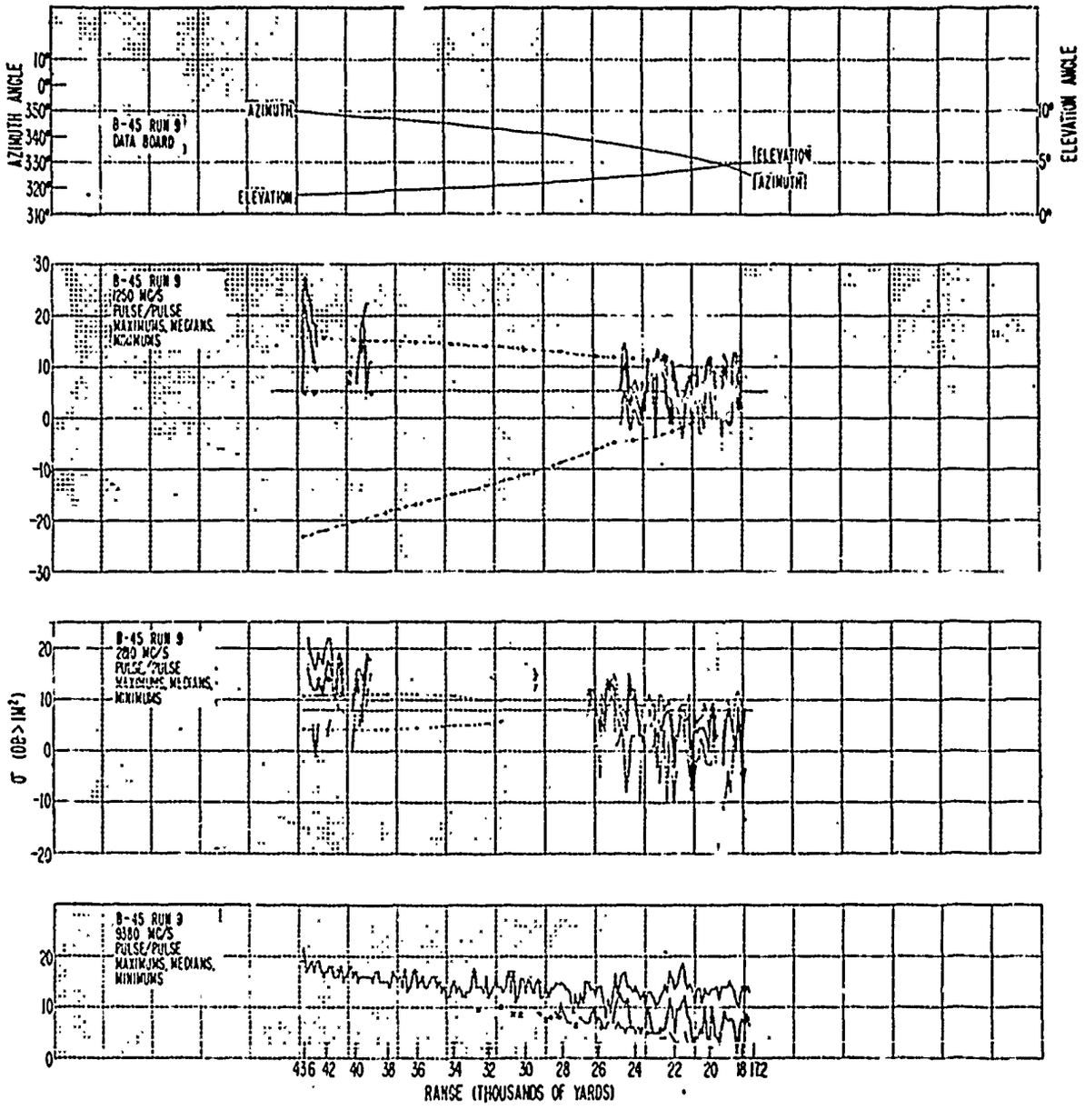
AZIMUTH ANGLE
ELEVATION ANGLE
B-45 RUN 9
DATA BOARD
AZIMUTH
ELEVATION
ELEVATION
AZIMUTH
B-45 RUN 9
1250 MC/S
PULSE/PULSE
MAXIMUMS, MEDIANS,
MINIMUMS
B-45 RUN 9
2800 MC/S
PULSE/PULSE
MAXIMUMS, MEDIANS,
MINIMUMS
σ (DB>1M²)
B-45 RUN 9
9380 MC/S
PULSE/PULSE
MAXIMUMS, MEDIANS,
MINIMUMS
RANGE (THOUSANDS OF YARDS)

Figure 9

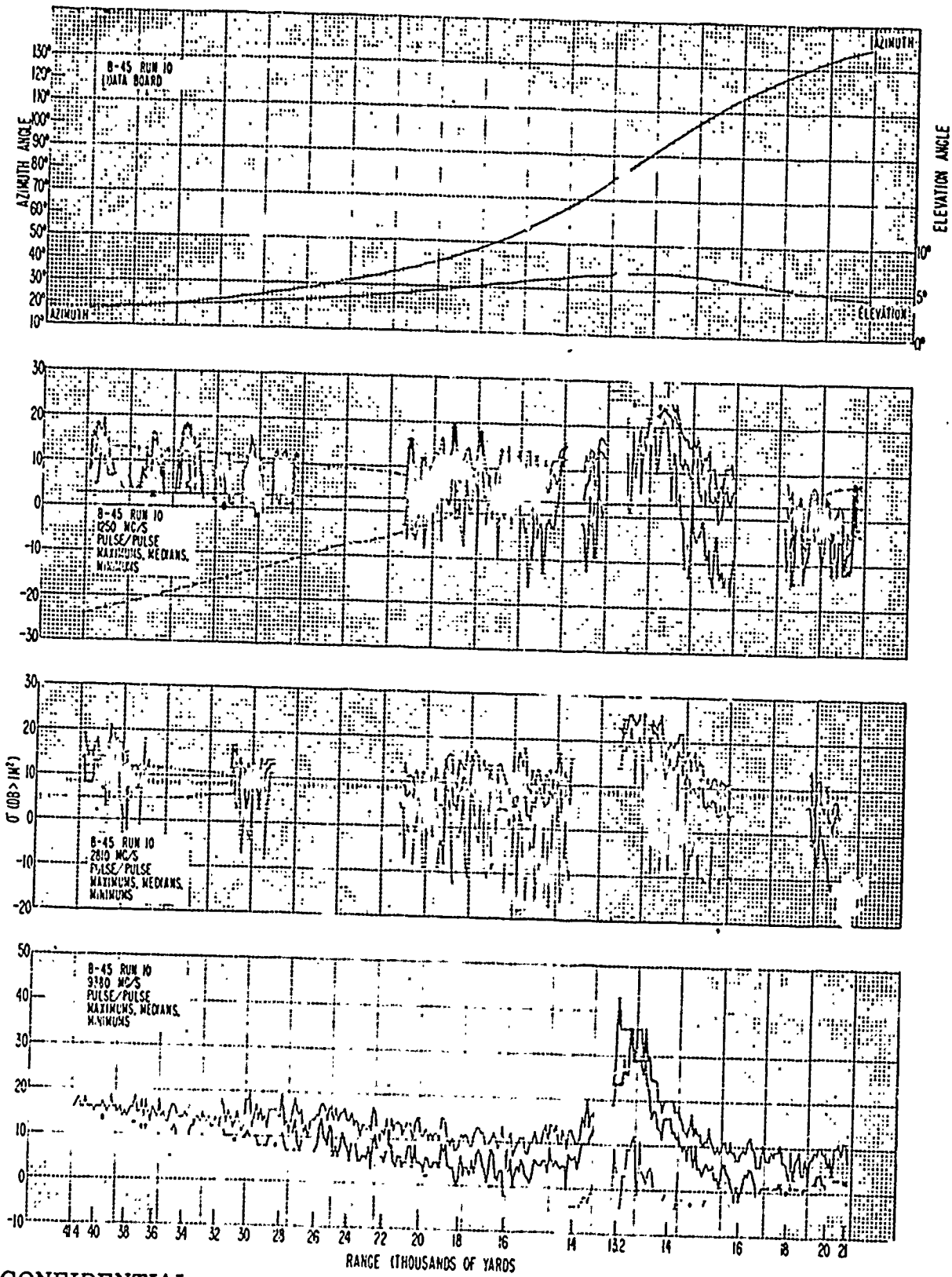
B-45 RUN 10
DATA BOARD
AZIMUTH ANGLE
ELEVATION ANGLE
AZIMUTH
ELEVATION
B-45 RUN 10
1250 MC/S
PULSE/PULSE
MAXIMUMS, MEDIANS,
MINIMUMS
σ (DB>1M²)
B-45 RUN 10
2810 MC/S
PULSE/PULSE
MAXIMUMS, MEDIANS,
MINIMUMS
B-45 RUN 10
9380 MC/S
PULSE/PULSE
MAXIMUMS, MEDIANS,
MINIMUMS
RANGE (THOUSANDS OF YARDS

Figure 10

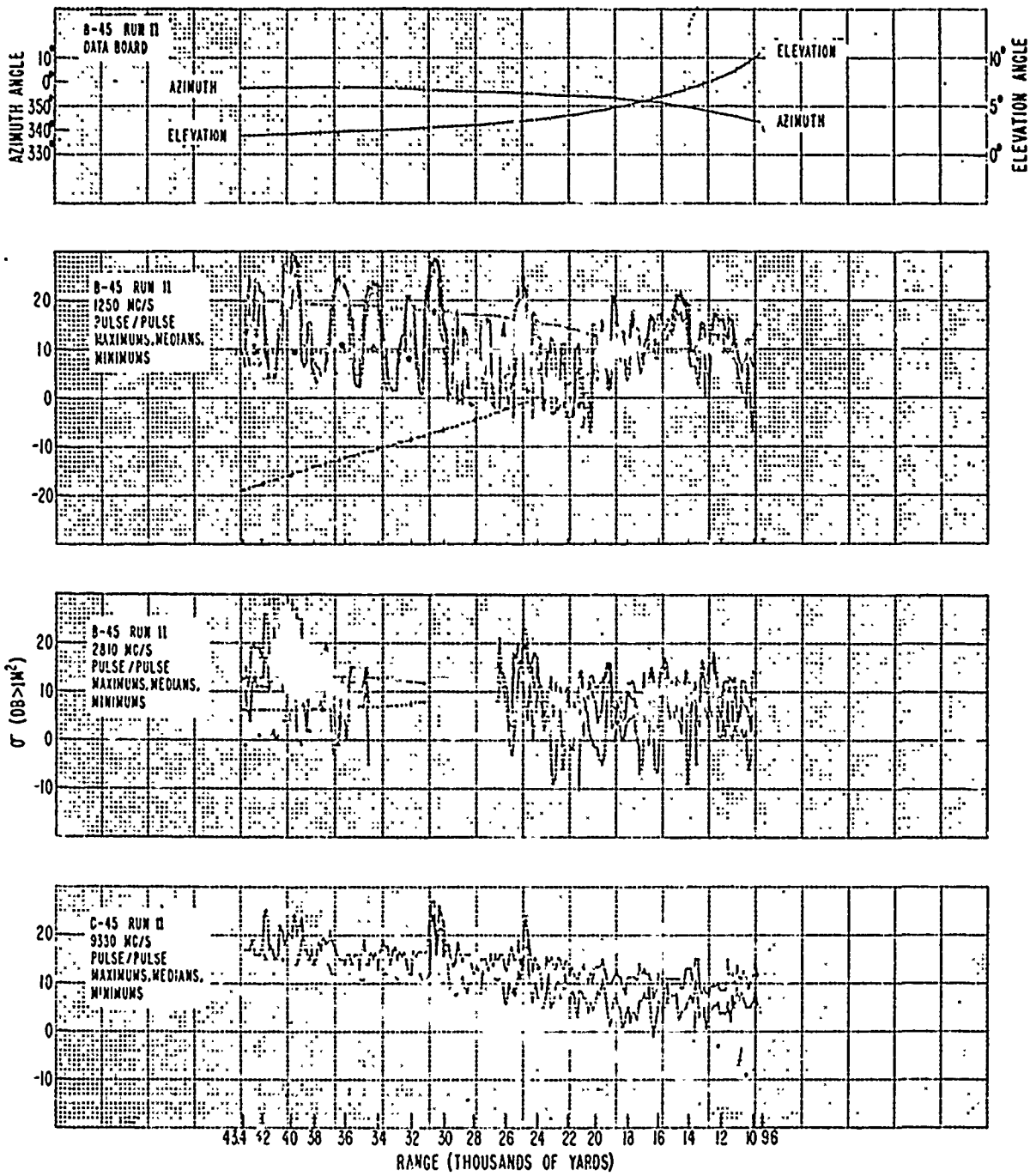
B-45 RUN 11
DATA BOARD
AZIMUTH
ELEVATION
AZIMUTH ANGLE
ELEVATION ANGLE
B-45 RUN 11
1250 MC/S
PULSE/PULSE
MAXIMUMS, MEDIANS,
MINIMUMS
B-45 RUN 11
2810 MC/S
PULSE/PULSE
MAXIMUMS, MEDIANS,
MINIMUMS
σ (DB>1M²)
C-45 RUN 11
9330 MC/S
PULSE/PULSE
MAXIMUMS, MEDIANS,
MINIMUMS
RANGE (THOUSANDS OF YARDS)

Figure 11

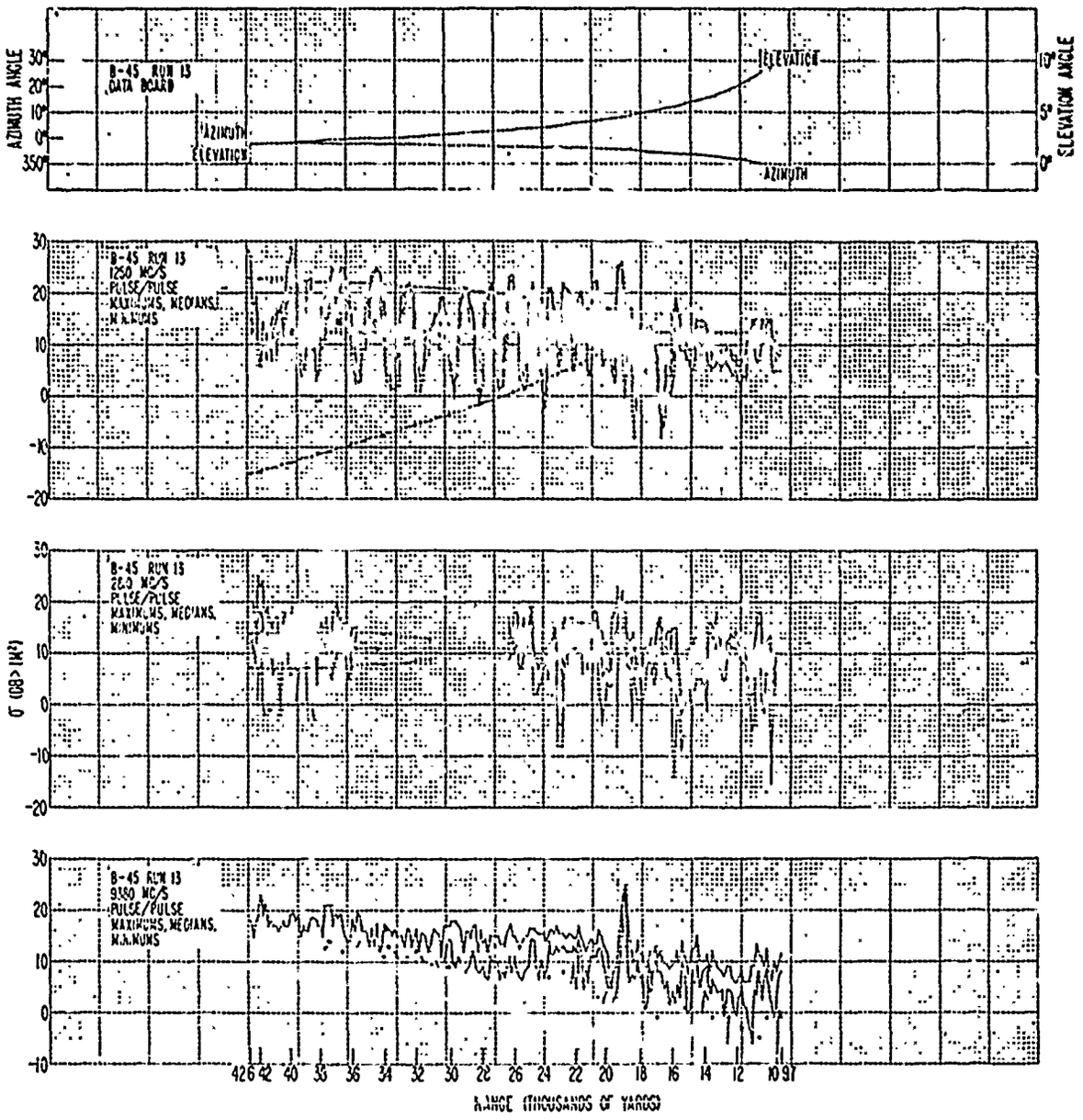
B-45 RUN 13
DATA BOARD
AZIMUTH
ELEVATION
AZIMUTH ANGLE
ELEVATION ANGLE
B-45 RUN 13
1250 MC/S
PULSE/PULSE
MAXIMUMS, MEDIANS,
MINIMUMS
B-45 RUN 13
2800 MC/S
PULSE/PULSE
MAXIMUMS, MEDIANS,
MINIMUMS
B-45 RUN 13
9350 MC/S
PULSE/PULSE
MAXIMUMS, MEDIANS,
MINIMUMS
σ (DB>1M²)
RANGE (THOUSANDS OF YARDS)

Figure 12

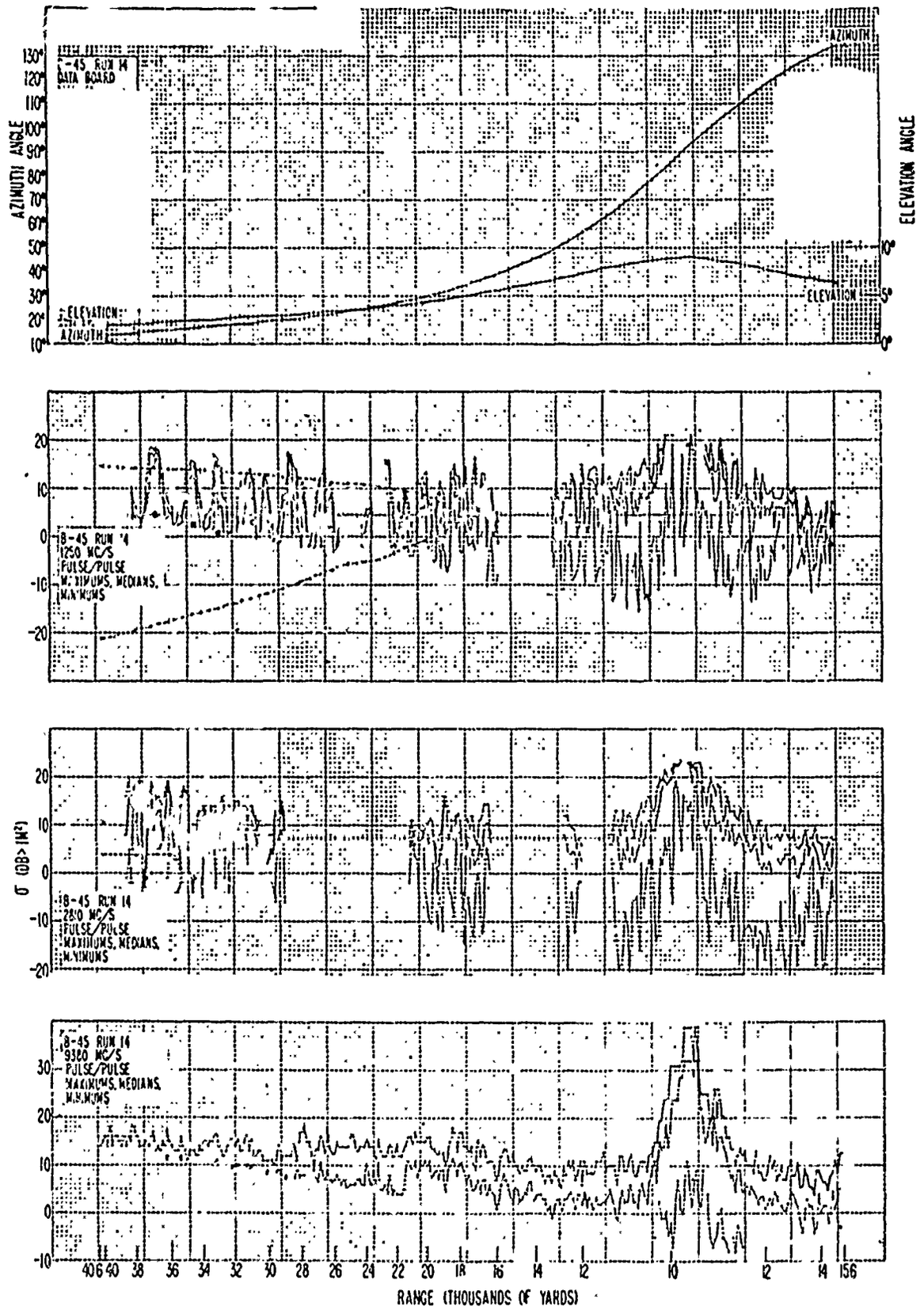
AZIMUTH ANGLE
ELEVATION ANGLE
AZIMUTH
ELEVATION
18-45 RUN 14
DATA BOARD
18-45 RUN 14
1250 MC/S
PULSE/PULSE
18-45 RUN 14
2810 MC/S
PULSE/PULSE
MAXIMUMS, MEDIANS, MINIMUMS
18-45 RUN 14
9380 MC/S
PULSE/PULSE
MAXIMUMS, MEDIANS, MINIMUMS
RANGE (THOUSANDS OF YARDS)

Figure 13

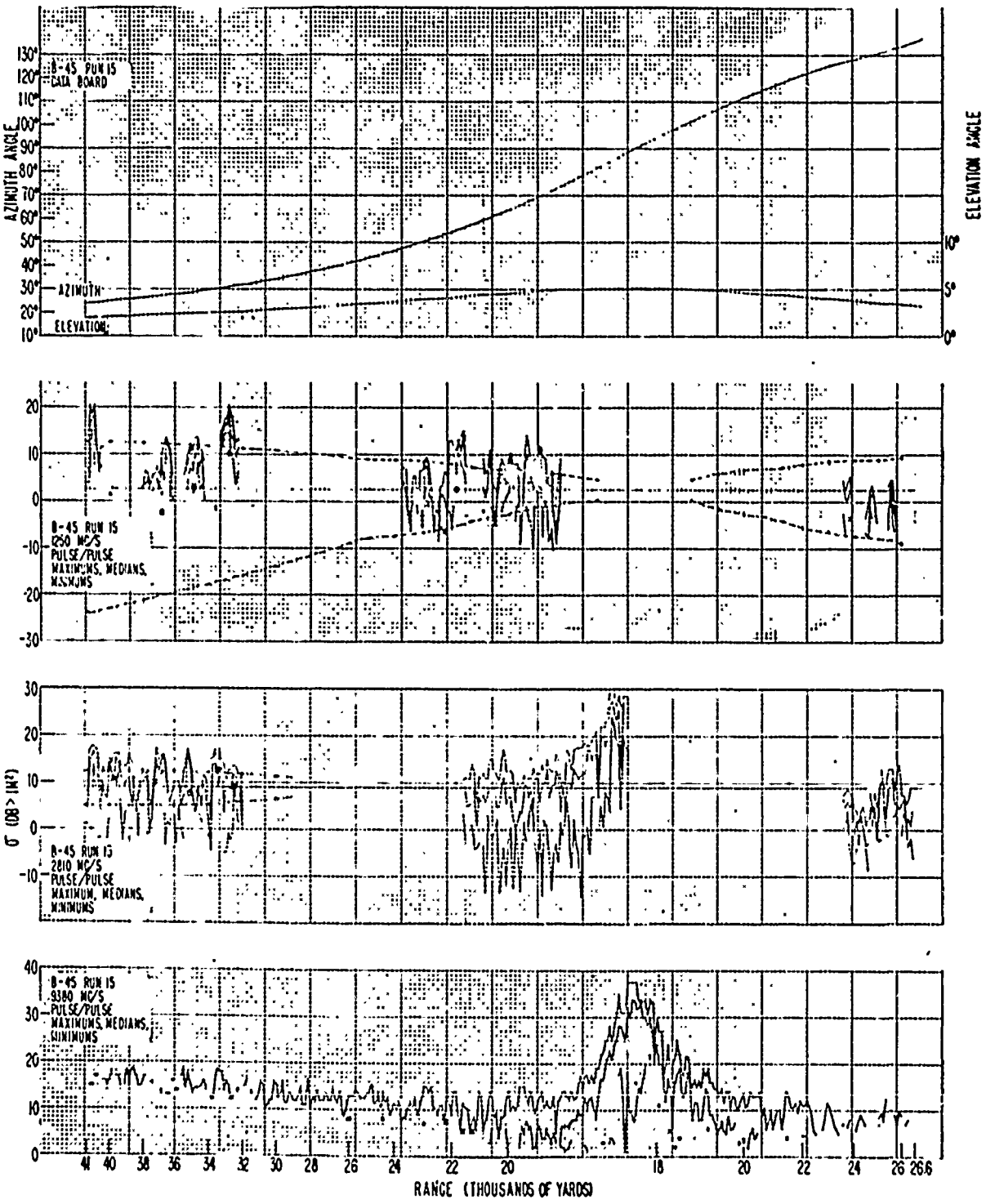
B-45 RUN 15
DATA BOARD
AZIMUTH ANGLE
ELEVATION ANGLE
AZIMUTH
ELEVATION
B-45 RUN 15
250 MC/S
PULSE/PULSE
MAXIMUMS, MEDIANS,
MINIMUMS
σ (DB > M²)
B-45 RUN 15
2810 MC/S
PULSE/PULSE
MAXIMUM, MEDIANS,
MINIMUMS
B-45 RUN 15
9380 MC/S
PULSE/PULSE
MAXIMUMS, MEDIANS,
MINIMUMS
RANGE (THOUSANDS OF YARDS)

Figure 14

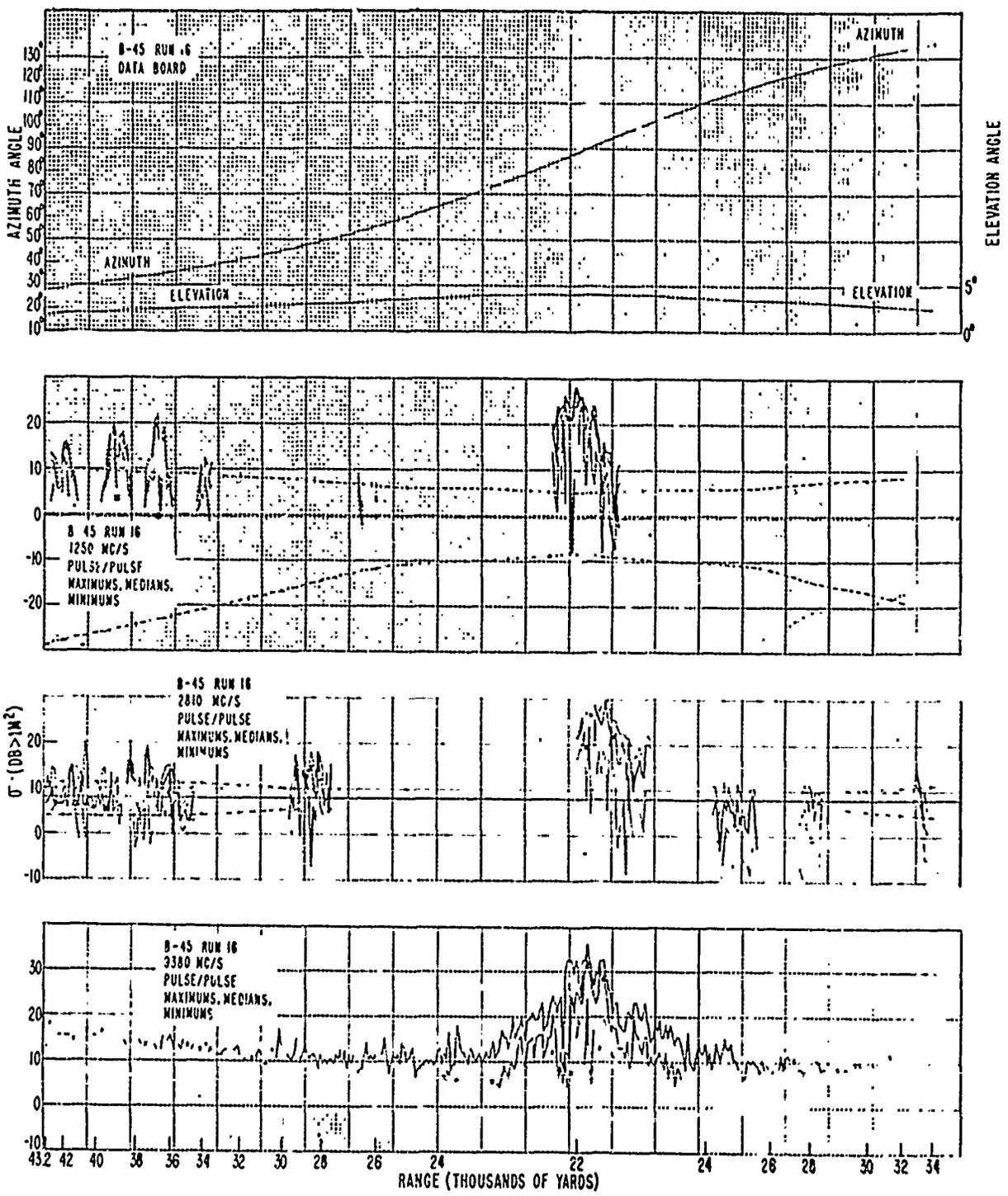
B-45 RUN 16
DATA BOARD
AZIMUTH
ELEVATION
AZIMUTH ANGLE
ELEVATION ANGLE
B 45 RUN 16
1250 MC/S
PULSE/PULSE
MAXIMUMS, MEDIANS,
MINIMUMS
B-45 RUN 16
2810 MC/S
PULSE/PULSE
MAXIMUMS, MEDIANS,
MINIMUMS
B-45 RUN 16
3380 MC/S
PULSE/PULSE
MAXIMUMS, MEDIANS,
MINIMUMS
RANGE (THOUSANDS OF YARDS)

Figure 15

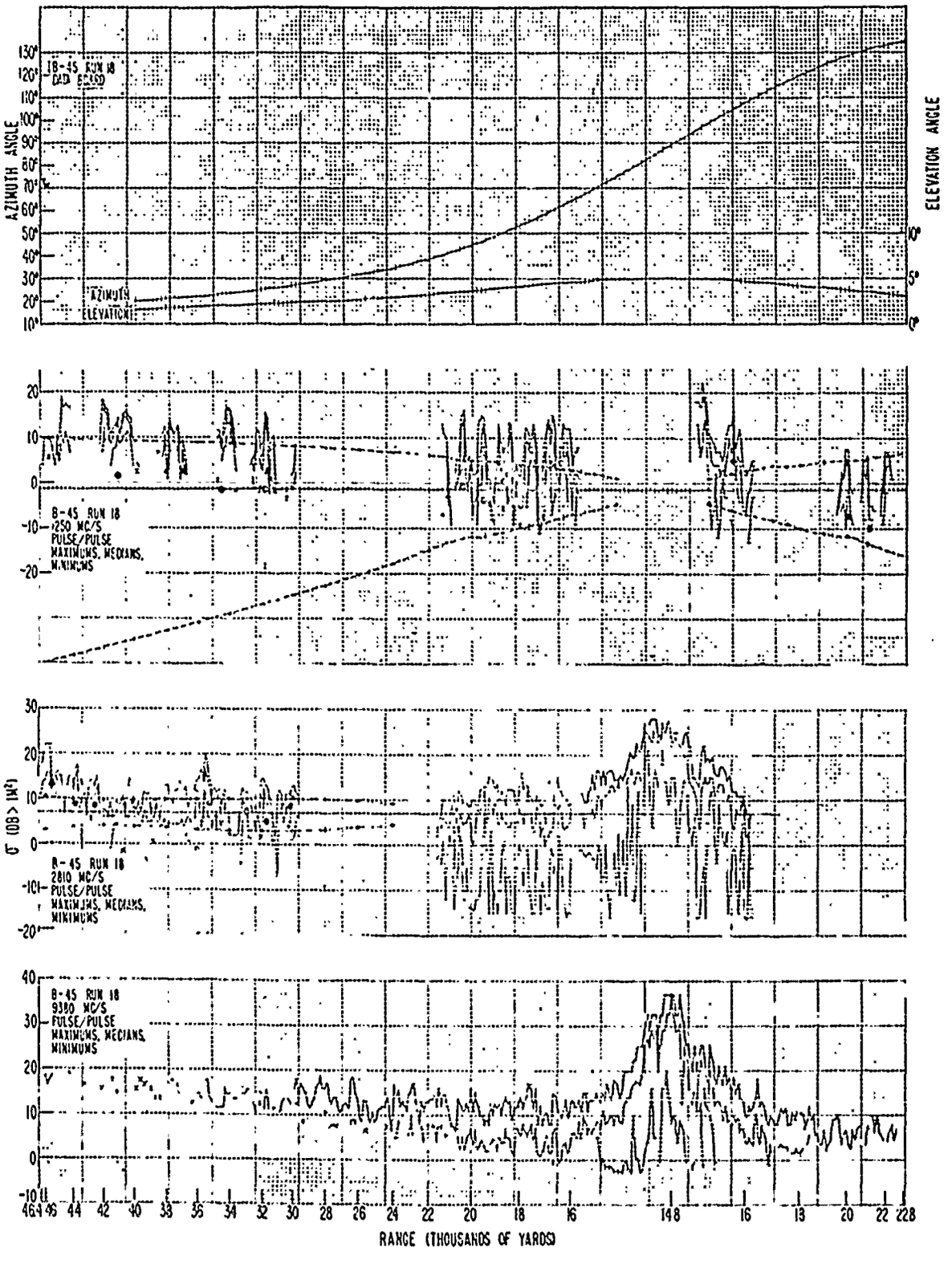
AZIMUTH ANGLE
ELEVATION ANGLE
B-45 RUN 18
DATA BOARD
AZIMUTH
ELEVATION
B-45 RUN 18
1250 MC/S
PULSE/PULSE
MAXIMUMS, MEDIANS,
MINIMUMS
B-45 RUN 18
2810 MC/S
PULSE/PULSE
MAXIMUMS, MEDIANS,
MINIMUMS
B-45 RUN 18
9380 MC/S
PULSE/PULSE
MAXIMUMS, MEDIANS,
MINIMUMS
RANGE (THOUSANDS OF YARDS)

Figure 16

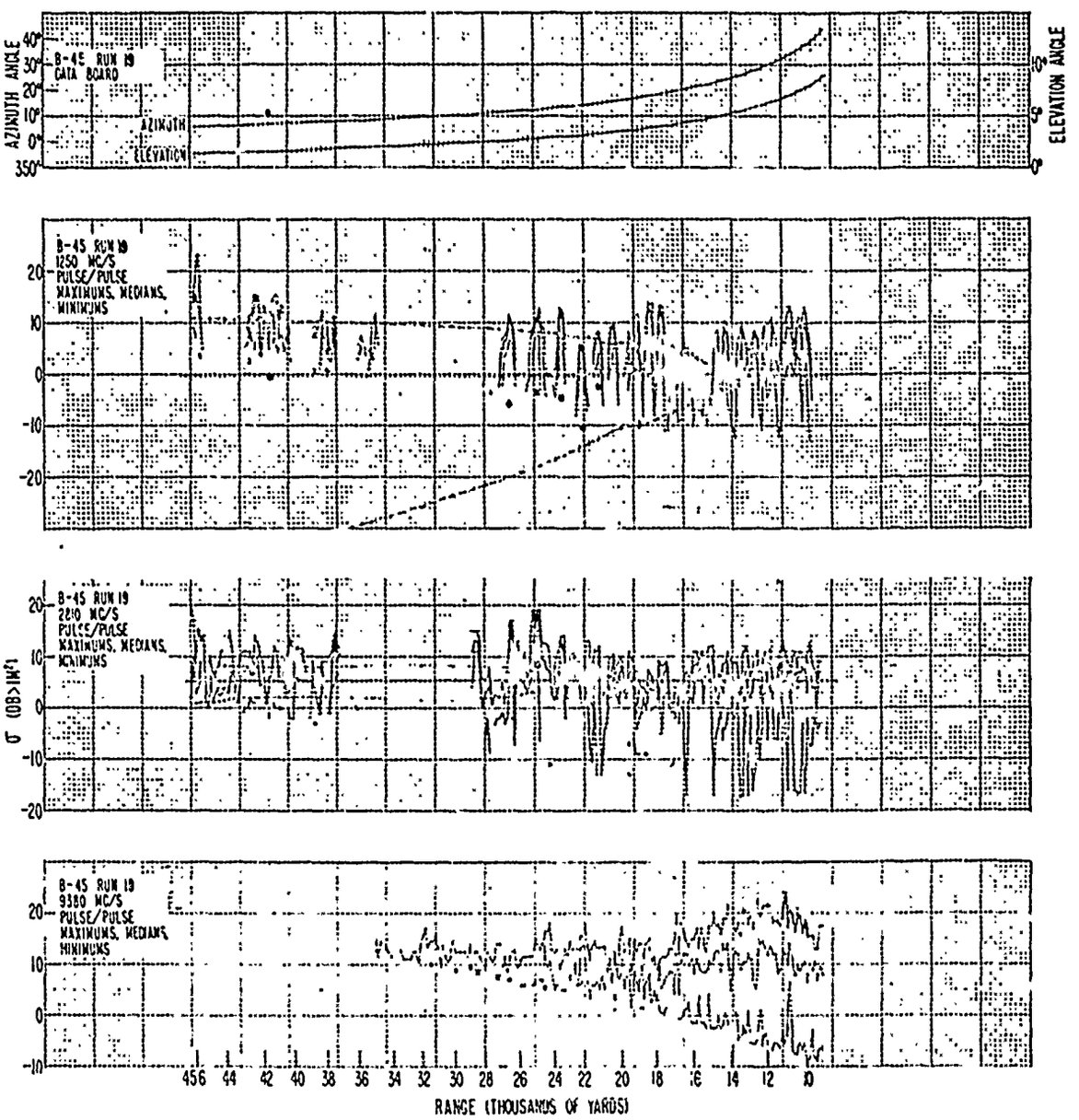
AZIMUTH ANGLE
ELEVATION ANGLE
B-45 RUN 19
DATA BOARD
AZIMUTH
ELEVATION
B-45 RUN 19
1250 MC/S
PULSE/PULSE
MAXIMUMS, MEDIANS,
MINIMUMS
B-45 RUN 19
2810 MC/S
PULSE/PULSE
MAXIMUMS, MEDIANS,
MINIMUMS
σ (DB>1M²)
B-45 RUN 19
9380 MC/S
PULSE/PULSE
MAXIMUMS, MEDIANS,
MINIMUMS
RANGE (THOUSANDS OF YARDS)

Figure 17

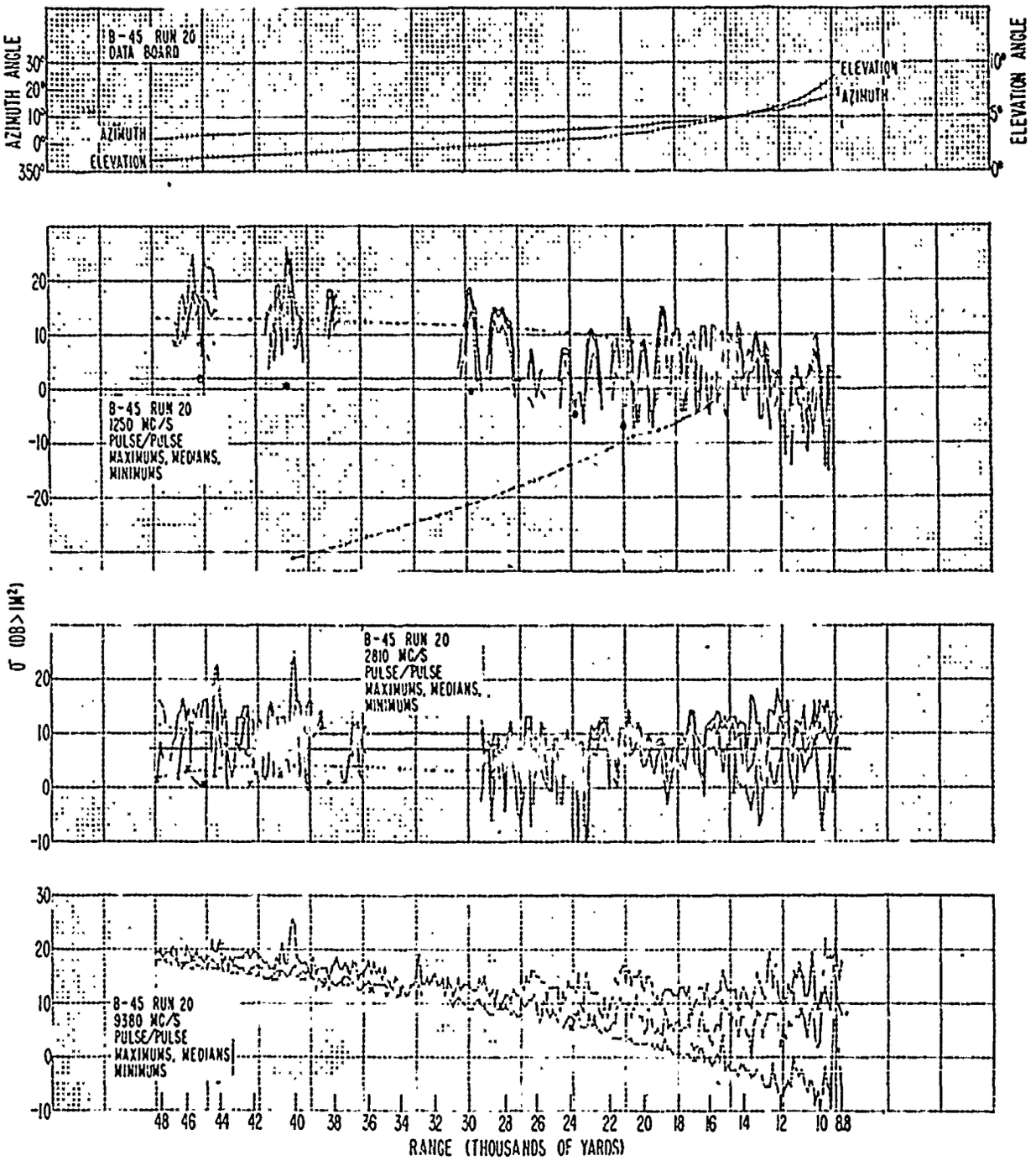
B-45 RUN 20
DATA BOARD
AZIMUTH ANGLE
ELEVATION ANGLE
AZIMUTH
ELEVATION
B-45 RUN 20
1250 MC/S
PULSE/PULSE
MAXIMUMS, MEDIANS,
MINIMUMS
σ (DB>1M²)
B-45 RUN 20
2810 MC/S
PULSE/PULSE
MAXIMUMS, MEDIANS,
MINIMUMS
B-45 RUN 20
9380 MC/S
PULSE/PULSE
MAXIMUMS, MEDIANS
MINIMUMS
RANGE (THOUSANDS OF YARDS)

Figure 18

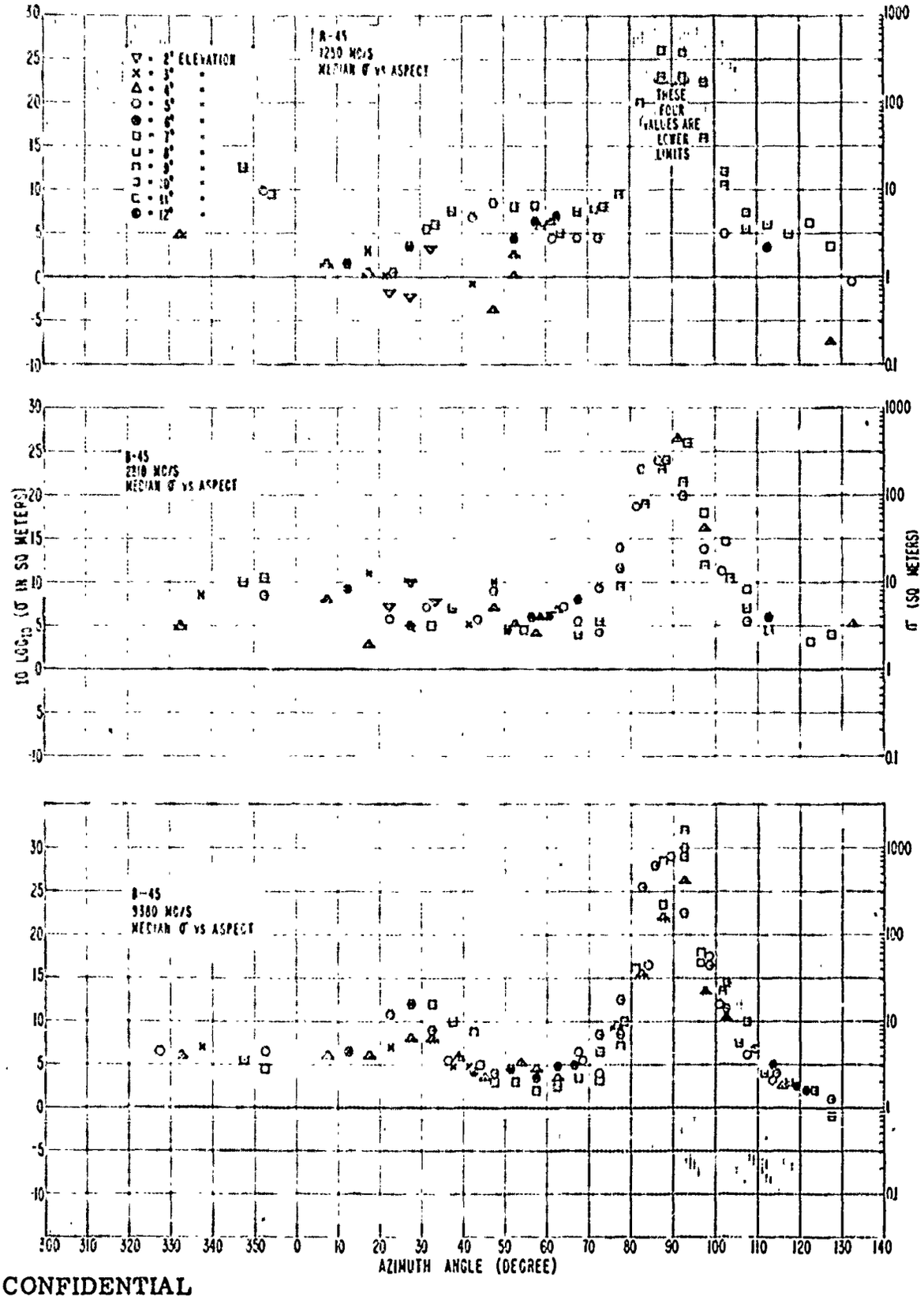
B-45
1250 MC/S
MEDIAN σ vs ASPECT
2° ELEVATION
THESE FOUR VALUES ARE LOWER LIMITS
B-45
2210 MC/S
MEDIAN σ vs ASPECT
10 LOG10 (σ IN SQ METERS)
σ (SQ METERS)
B-45
9380 MC/S
MEDIAN σ vs ASPECT
AZIMUTH ANGLE (DEGREE)

Figure 19

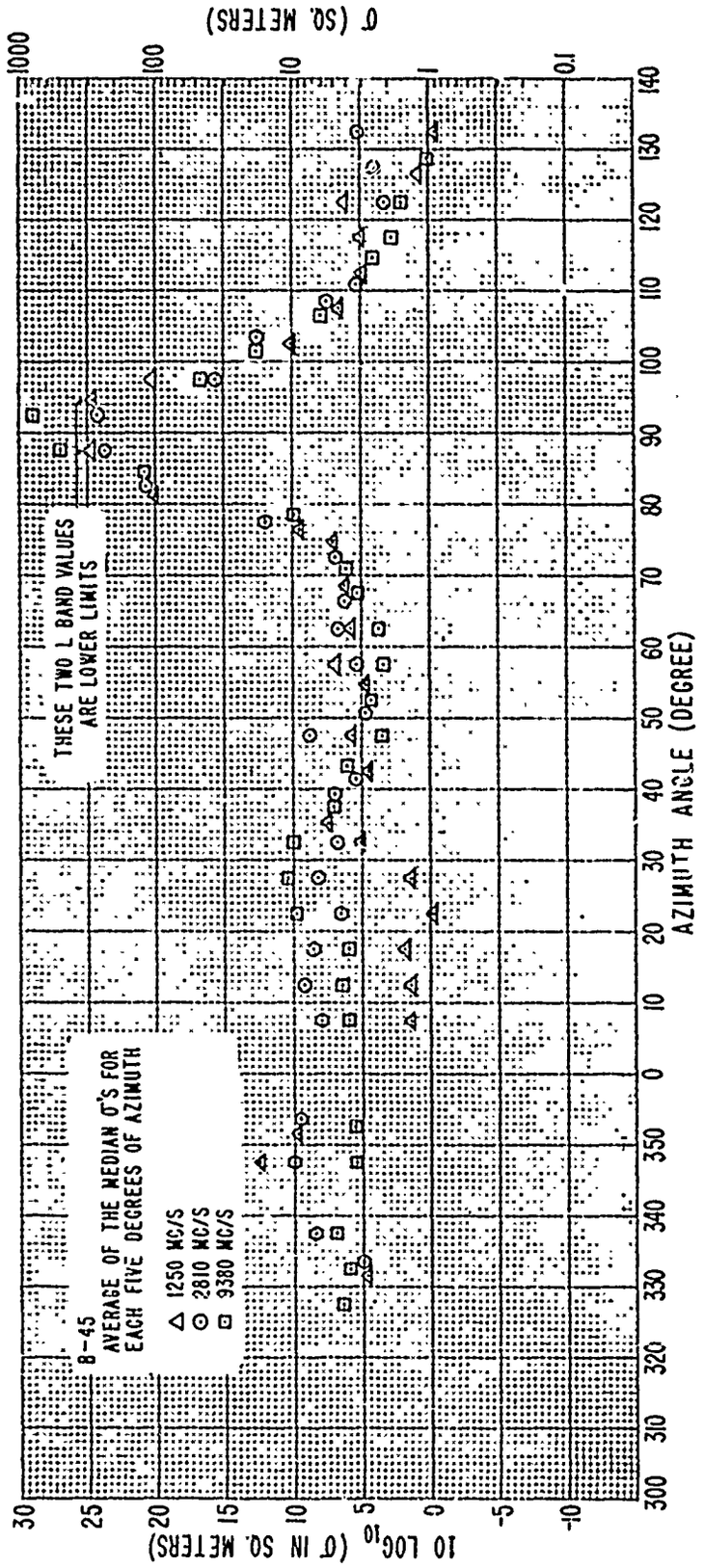
σ (SQ. METERS)
1000
100
10
1
0.1
THESE TWO L BAND VALUES ARE LOWER LIMITS
8-45
AVERAGE OF THE MEDIAN σ'S FOR EACH FIVE DEGREES OF AZIMUTH
△ 1250 MC/S
○ 2810 MC/S
□ 9380 MC/S
AZIMUTH ANGLE (DEGREE)
10 LOG10 (σ IN SQ. METERS)

Figure 20

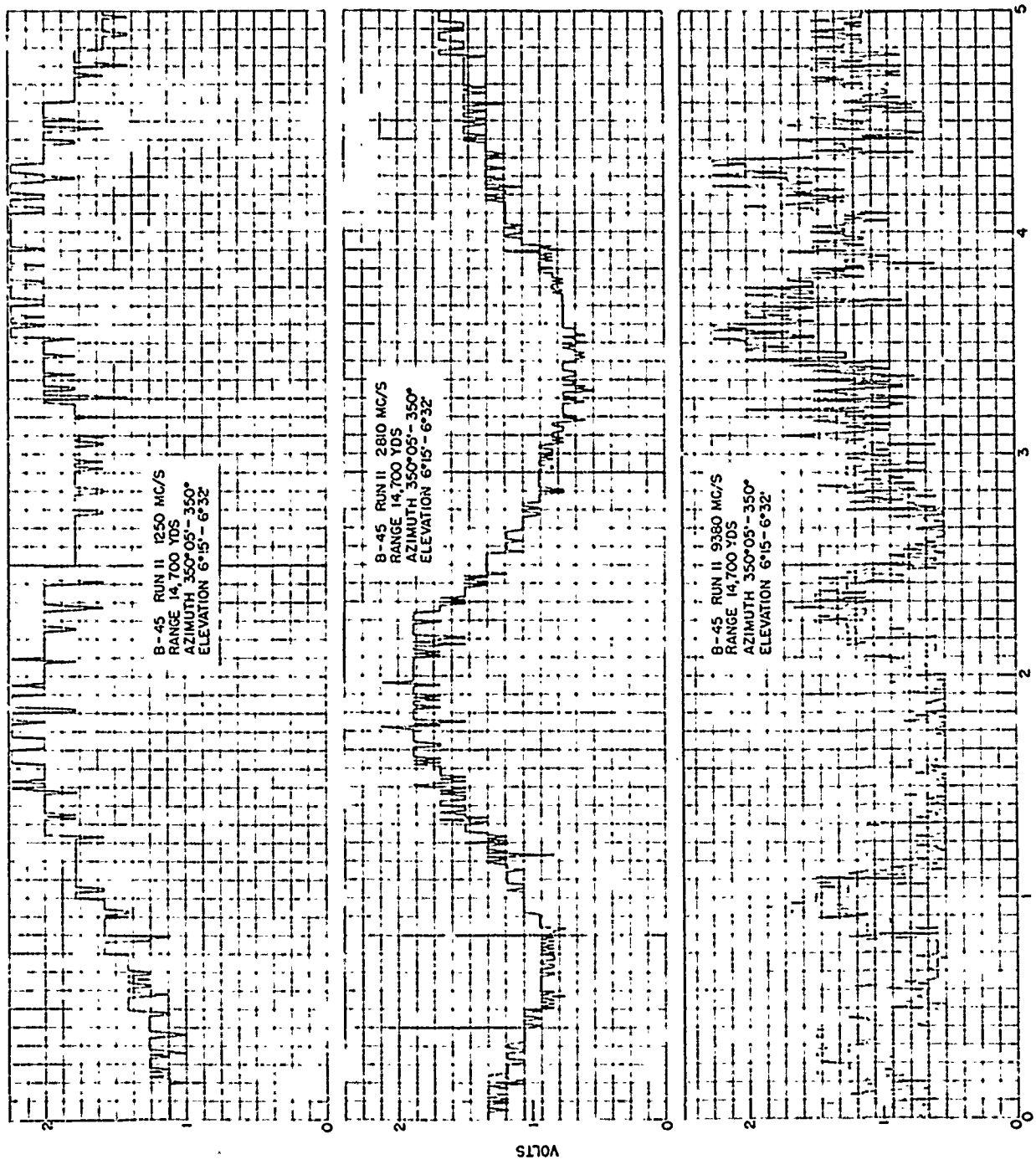
B-45 RUN 11 1250 MC/S
RANGE 14,700 YDS
AZIMUTH 350°05'-350°
ELEVATION 6°15'-6°32'
B-45 RUN 11 2810 MC/S
RANGE 14,700 YDS
AZIMUTH 350°05'-350°
ELEVATION 6°15'-6°32'
B-45 RUN 11 9380 MC/S
RANGE 14,700 YDS
AZIMUTH 350°05'-350°
ELEVATION 6°15'-6°32'
VOLTS
0
1
2
3
4
5

Figure 21

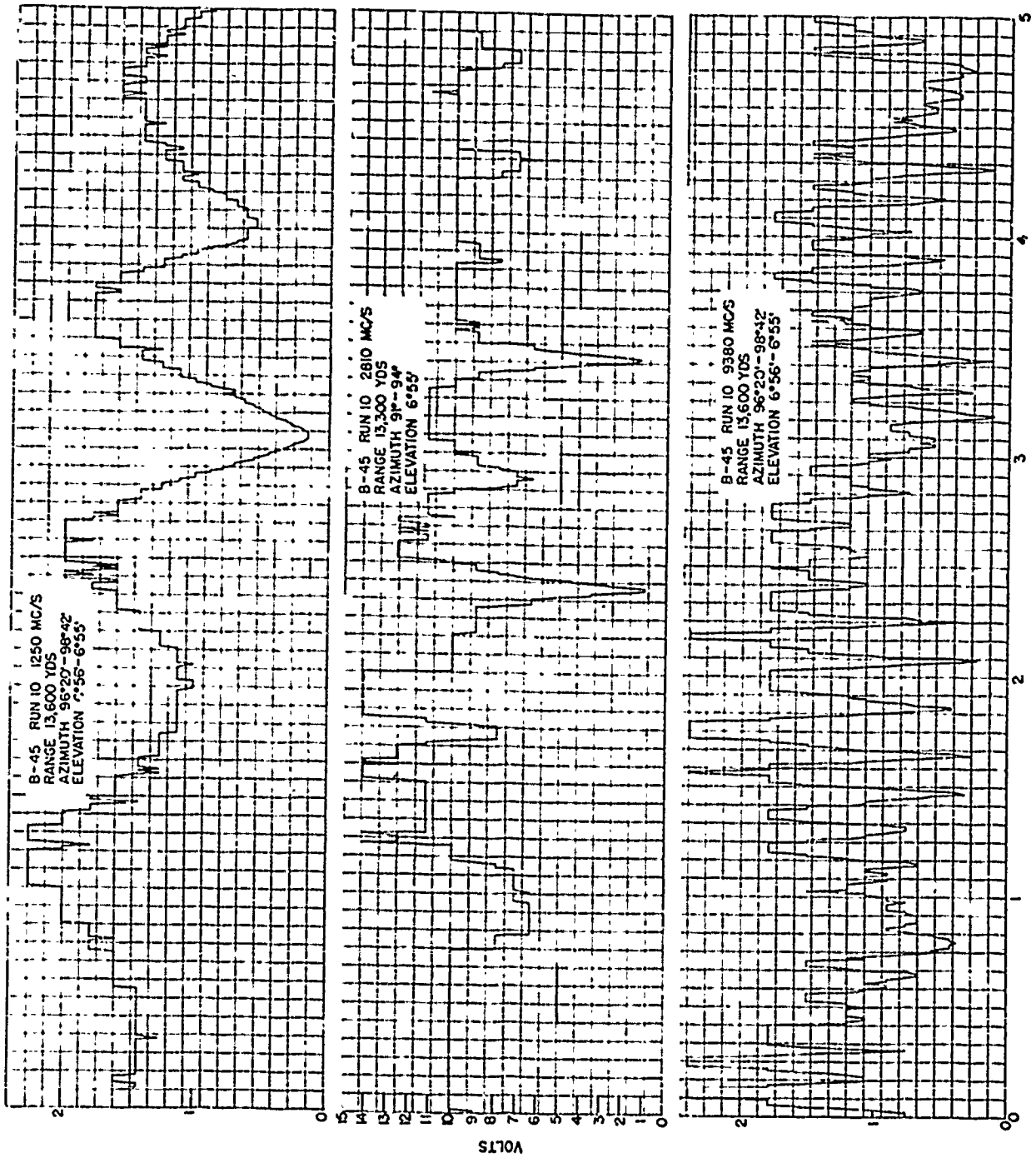
B-45 RUN 10 1250 MC/S
RANGE 13,600 YDS
AZIMUTH 96°20'-98°42'
ELEVATION 6°56'-6°55'
B-45 RUN 10 2810 MC/S
RANGE 13,300 YDS
AZIMUTH 91°-94°
ELEVATION 6°55'
B-45 RUN 10 9380 MC/S
RANGE 13,600 YDS
AZIMUTH 96°20'-98°42'
ELEVATION 6°56'-6°55'
VOLTS
TIME (SEC)

Figure 22

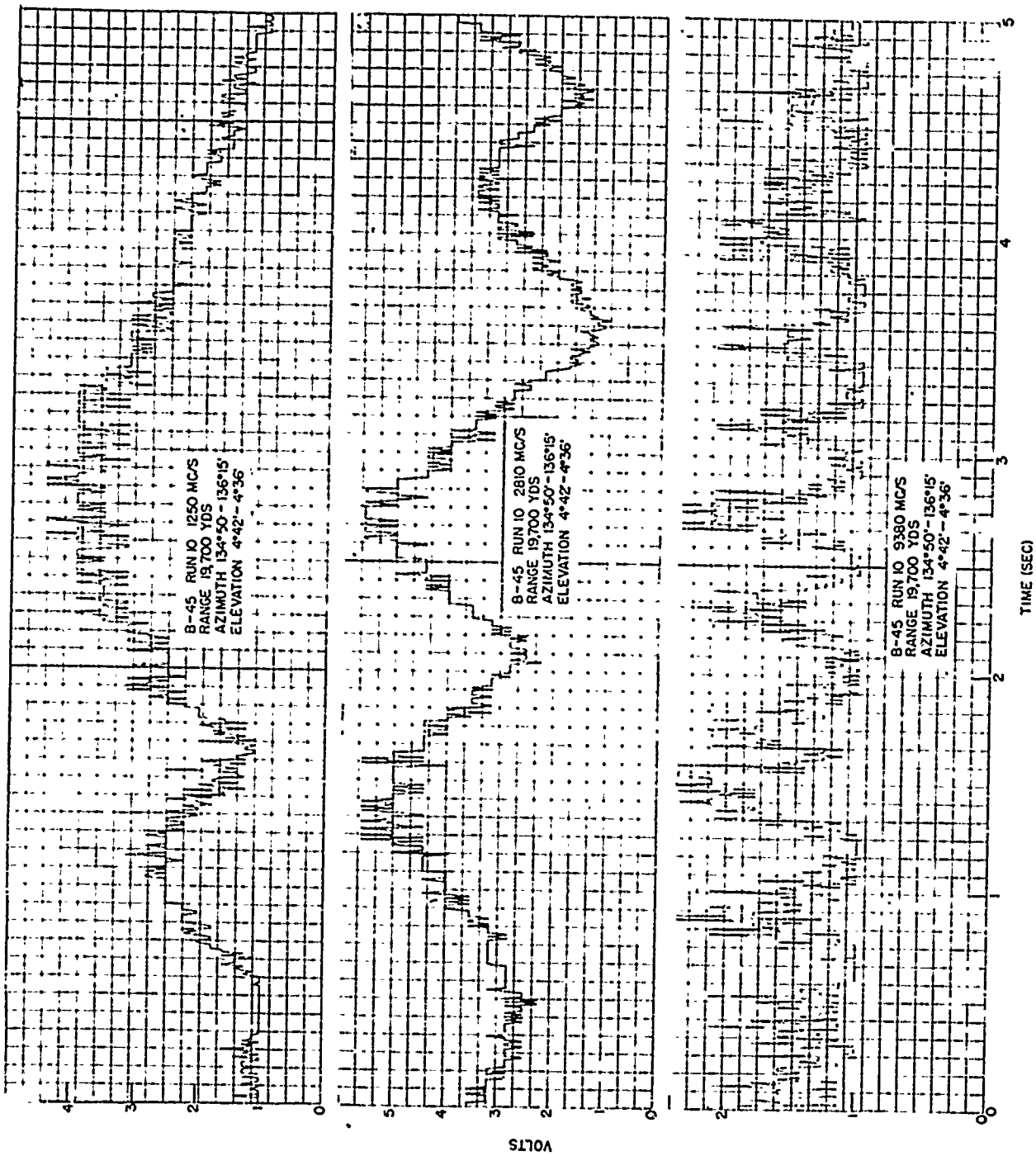

SECURITY INFORMATION

Figure 23

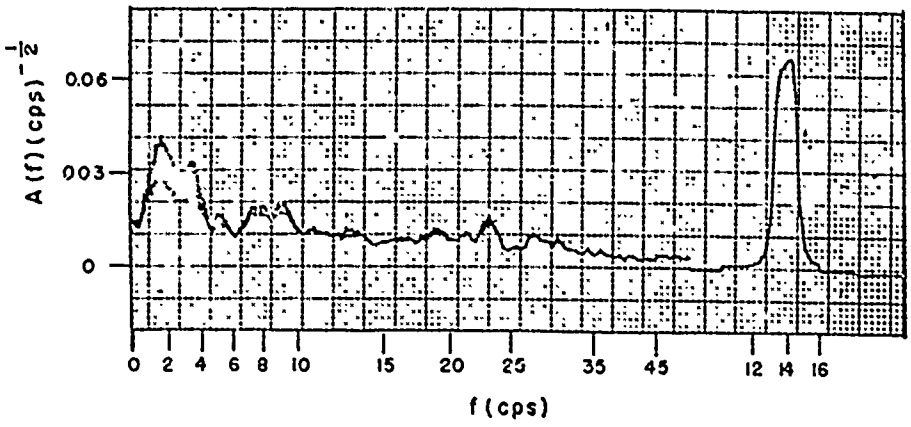

B-45 RUN 11 1250 MC/S
RANGE 14,700 YDS
AZIMUTH 350°05' - 350°
ELEVATION 6°15' - 6°32'

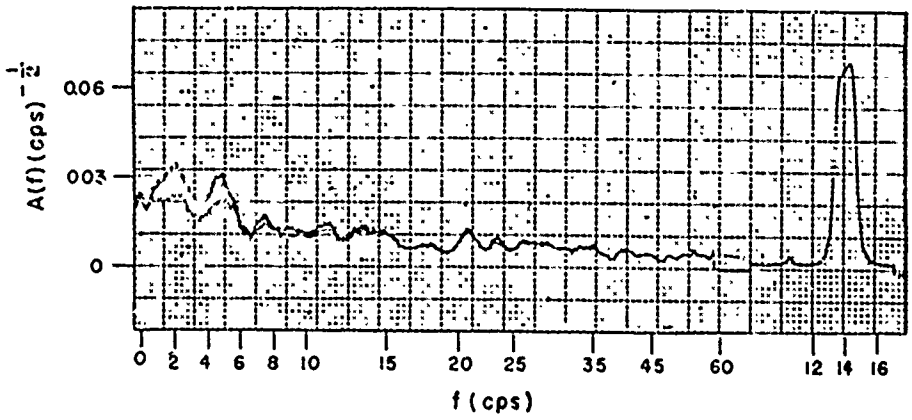

B-45 RUN 11 2810 MC/S
RANGE 14,700 YDS
AZIMUTH 350°05' - 350°
ELEVATION 6°15' - 6°32'

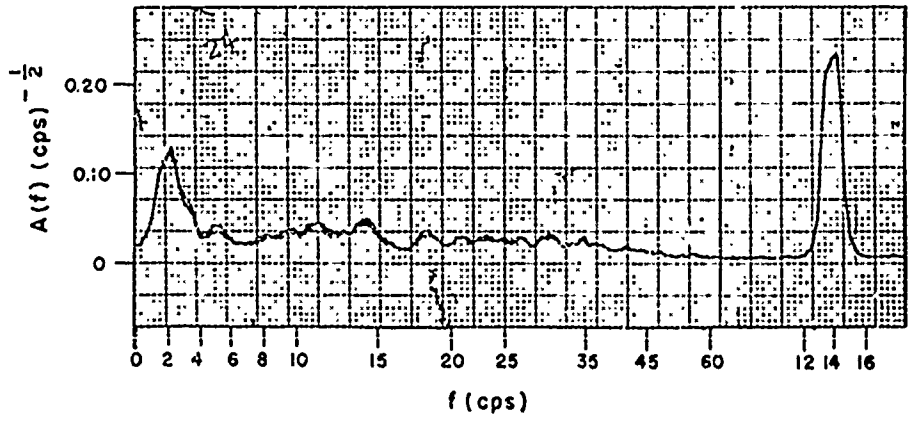

B-45 RUN 11 9380 MC/S
RANGE 14,700 YDS
AZIMUTH 350°05' - 350°07'
ELEVATION 6°15' - 6°32'

Figure 24

[redacted]

UNCLASSIFIED

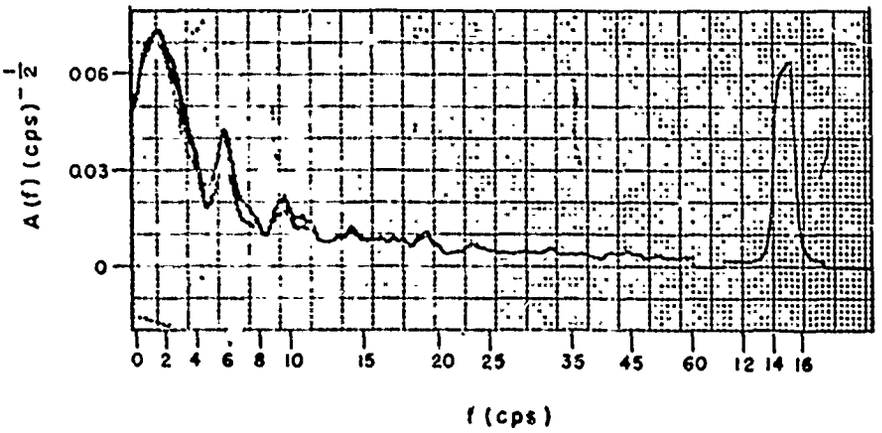

B-45 RUN 10 1250 MC/S
RANGE 13,600 YDS
AZIMUTH 96°20' - 98°42'
ELEVATION 6°56' - 6°55'

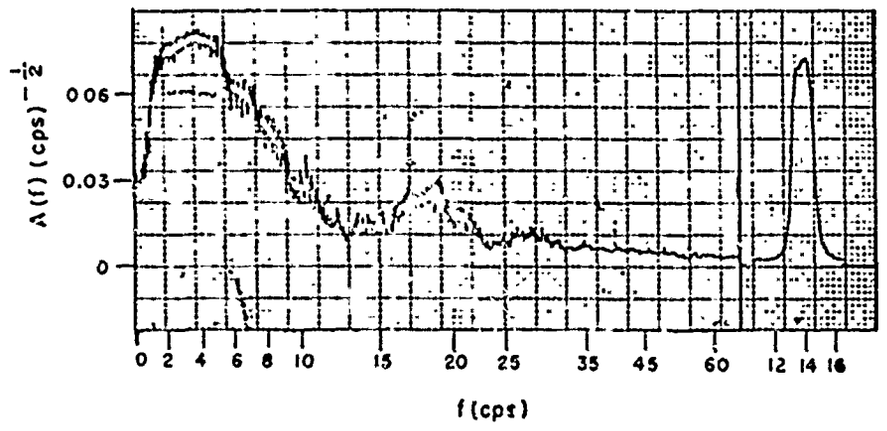

B-45 RUN 10 2810 MC/S
RANGE 13,300 YDS
AZIMUTH 91° - 94°
ELEVATION 6°55'

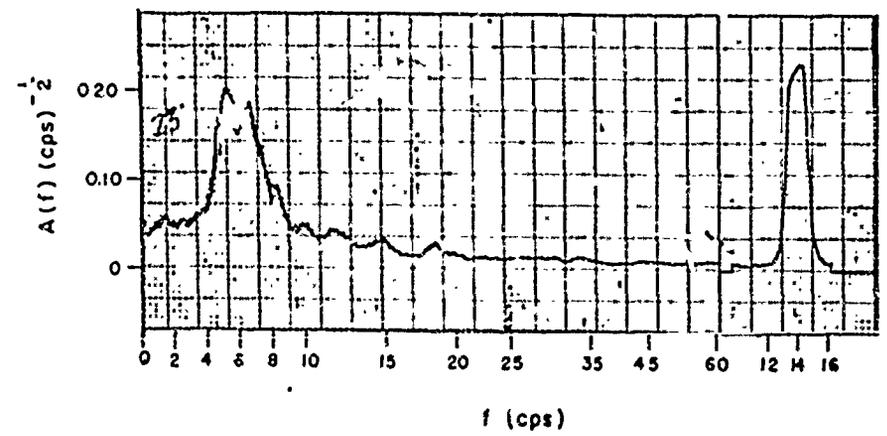

B-45 RUN 10 9380 MC/S
RANGE 13,600 YDS
AZIMUTH 96°20' - 98°42'
ELEVATION 6°56' - 6°55'

[redacted]

SECURITY INFORMATION.

Figure 25

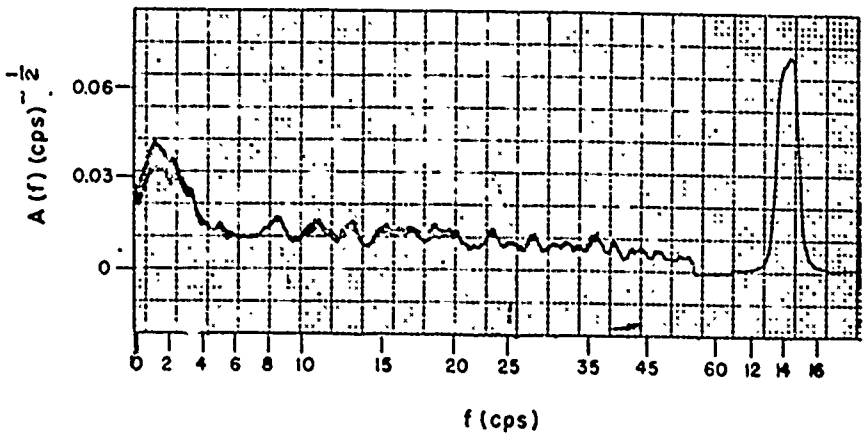

B-45 RUN 10 1250 MC/S
RANGE 19,700 YDS
AZIMUTH 134°50' - 136°15'
ELEVATION 4°42' - 4°36'

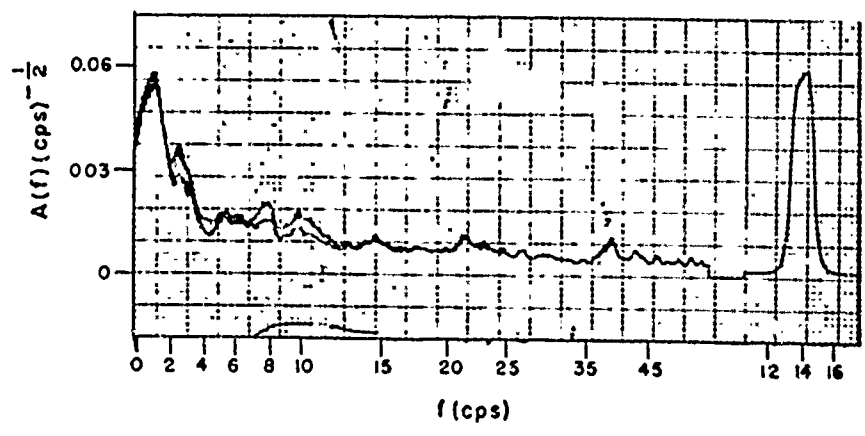

B-45 RUN 10 2810 MC/S
RANGE 19,700 YDS
AZIMUTH 134°50' - 136°15'
ELEVATION 4°42' - 4°36'

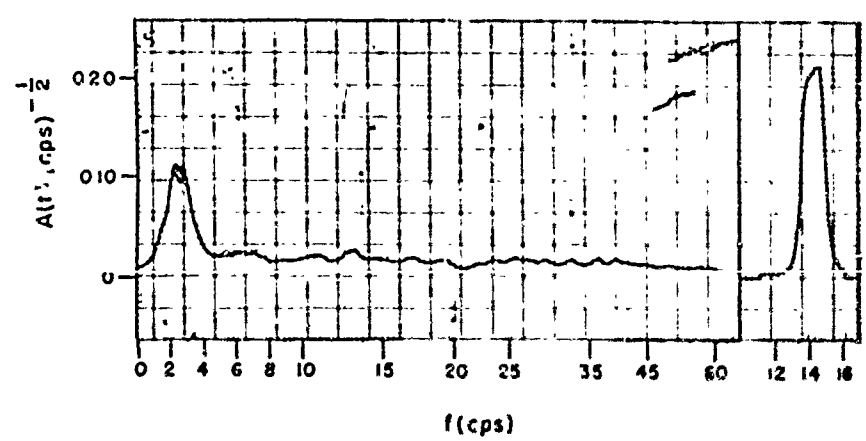

B-45 RUN 10 9380 MC/S
RANGE 19,700 YDS
AZIMUTH 134°50' - 136°15'
ELEVATION 4°42' - 4°36'

Figure 26